

AD _____

Award Number: DAMD17-00-C-0031

TITLE: Modeling for Military Operational Medicine Scientific and Technical Objectives (Articulated Human Biomechanical Modeling Toolbox) (Part I: Overview, Rigid Body Formulations, and Examples)

PRINCIPAL INVESTIGATOR: James H. Stuhmiller, Ph.D.
Weixin Shen

CONTRACTING ORGANIZATION: Jaycor, Incorporated
San Diego, California 92121-1002

REPORT DATE: December 2000

TYPE OF REPORT: Final, Part I

PREPARED FOR: U.S. Army Medical Research and Materiel Command
Fort Detrick, Maryland 21702-5012

DISTRIBUTION STATEMENT: Approved for Public Release;
Distribution Unlimited

The views, opinions and/or findings contained in this report are those of the author(s) and should not be construed as an official Department of the Army position, policy or decision unless so designated by other documentation.

20011005 296

REPORT DOCUMENTATION PAGE

Form Approved
OMB No. 074-0188

Public reporting burden for this collection of information is estimated to average 1 hour per response, including the time for reviewing instructions, searching existing data sources, gathering and maintaining the data needed, and completing and reviewing this collection of information. Send comments regarding this burden estimate or any other aspect of this collection of information, including suggestions for reducing this burden to Washington Headquarters Services, Directorate for Information Operations and Reports, 1215 Jefferson Davis Highway, Suite 1204, Arlington, VA 22202-4302, and to the Office of Management and Budget, Paperwork Reduction Project (0704-0188), Washington, DC 20503

1. AGENCY USE ONLY (Leave blank)	2. REPORT DATE December 2000	3. REPORT TYPE AND DATES COVERED Final, Part I ()
---	--	--

4. TITLE AND SUBTITLE Modeling for Military Operational Medicine Scientific and Technical Objectives (Articulated Human Biomechanical Modeling Toolbox) (Part I: Overview, Rigid Body Formulations, and Examples)	5. FUNDING NUMBERS DAMD17-00-1-0031
---	---

6. AUTHOR(S) James H. Stuhmiller, Ph.D. Weixin Shen
--

7. PERFORMING ORGANIZATION NAME(S) AND ADDRESS(ES) Jaycor, Incorporated San Diego, California 92121-1002 E-Mail:	8. PERFORMING ORGANIZATION REPORT NUMBER
--	---

9. SPONSORING / MONITORING AGENCY NAME(S) AND ADDRESS(ES) U.S. Army Medical Research and Materiel Command Fort Detrick, Maryland 21702-5012	10. SPONSORING / MONITORING AGENCY REPORT NUMBER
--	---

11. SUPPLEMENTARY NOTES Report contains color.
--

12a. DISTRIBUTION / AVAILABILITY STATEMENT Approved for Public Release; Distribution Unlimited.	12b. DISTRIBUTION CODE
---	-------------------------------

13. ABSTRACT (Maximum 200 Words)

14. SUBJECT TERMS	15. NUMBER OF PAGES 51
	16. PRICE CODE

17. SECURITY CLASSIFICATION OF REPORT Unclassified	18. SECURITY CLASSIFICATION OF THIS PAGE Unclassified	19. SECURITY CLASSIFICATION OF ABSTRACT Unclassified	20. LIMITATION OF ABSTRACT Unlimited
--	---	--	--



J00-3150.31-135

Articulated Human Biomechanical Modeling Toolbox

Part I: Overview, Rigid Body Formulations, and Examples

Prepared by:

Weixin Shen
Jaycor, Inc.
3394 Carmel Mountain Road
San Diego, California 92121-1002

Prepared for:

Commander
U.S. Army Medical Research and Materiel Command
Ft. Detrick, Maryland 21702-5012

Contract No. DAMD17-00-C-0031

December 2000

JAYCOR

ABSTRACT

In the first phase of the project to develop an articulated human biomechanical modeling toolbox (AHBM), efforts were made to review the current status of modeling techniques and to develop rigid body formulations suitable for human biomechanical modeling. The developed version-one of the toolbox, AHBM V1, consists of kinematics, inverse and forward dynamics algorithms, data conversion routines, graphical algorithms, and many utility routines for mathematical calculation and file operation. Both inverse and forward sample models, such as a 3D lower extremity model, a 3D whole body human model, and a human head-neck model, were developed. AHBM V1 was also used for two application projects: upgrading gait analysis software for USARIEM; and developing a new method to understand the airbag external load behavior and bag-occupant interaction for Department of Transportation.

The following specific tasks were completed in the first phase

- ◆ Review of current techniques for human biomechanical modeling
- ◆ Developing three-dimensional kinematics algorithms
- ◆ Developing forward dynamics formulations for multibody constrained systems
- ◆ Developing commonly used algorithms related to inverse dynamics analysis
- ◆ Developing data structure and data conversion routines
- ◆ Developing some graphical algorithms for visualizing data and model
- ◆ Developing utility routines for mathematical calculation and file operation
- ◆ Developing example problems for both inverse and forward dynamics analysis

In the phase two of the project, efforts will be focused on reviewing and developing muscle models. The muscle models will be included in AHBM V2. This will expand the toolbox's capabilities to handle human biomechanical modeling where muscle activities have to be accounted for. Specific applications may include solving muscle load sharing in inverse dynamics analysis and understanding overuse injuries related to muscle activities.

This report is separated into two parts. The first part consists of an overview of the toolbox, rigid body formulations, and example models and applications. The second part provides detailed description of individual routines in the toolbox.

TABLE OF CONTENTS

	<u>Page</u>
1 OVERVIEW.....	1
1.1 INTRODUCTION.....	1
1.2 BIOMECHANICAL ANALYSIS, MODELING AND SIMULATION.....	1
<i>Need for Biomechanical Modeling</i>	1
<i>Model Sub-systems</i>	2
<i>Types of Biomechanical Analysis and Modeling</i>	3
1.3 DEVELOPING A BIOMECHANICAL MODELING TOOLBOX.....	6
2 MULTIBODY KINEMATICS.....	11
2.1 TREE STRUCTURED MULTIBODY SYSTEM.....	11
2.2 REPRESENTATION OF RIGID BODY ORIENTATION.....	13
<i>Rotational (Orientation) Matrix</i>	13
<i>Euler Angles</i>	14
<i>Euler Parameters</i>	16
2.3 ANGULAR VELOCITY AND ACCELERATION.....	17
2.4 TRACKING TUMBLING MOTION.....	18
2.5 LINEAR POSITION, VELOCITY AND ACCELERATION.....	19
2.6 CONSTRAINTS.....	19
3 FORWARD DYNAMICS FORMULATION.....	25
3.1 GOVERNING EQUATION.....	25
3.2 NUMERICAL FORMULATION.....	27
3.3 PROJECTION OF POSITION AND VELOCITY CONSTRAINTS.....	27
<i>Projection of Position Constraint</i>	27
<i>Projection of Velocity Constraint</i>	28
4 INVERSE DYNAMICS ANALYSIS.....	29
4.1 MEASURING KINEMATIC DATA AND GROUND REACTION FORCE.....	29
4.2 KINEMATICS RECONSTRUCTION.....	29
4.3 BODY SEGMENT PARAMETERS.....	30
4.4 JOINT DYNAMICS FORMULATION.....	31
5 EXAMPLES AND APPLICATIONS.....	33
5.1 INVERSE DYNAMICS EXAMPLES AND APPLICATIONS.....	33
<i>Gait3D V1 Developed for USAREIM</i>	33
<i>Inverse Dynamics Model for Predicting Airbag Forces</i>	35
<i>A three-dimensional lower extremity model</i>	36
5.2 FORWARD DYNAMICS ANALYSIS EXAMPLES.....	38
<i>Simple Spring Mass Model</i>	38
<i>Three-dimensional Double Pendulums</i>	39
<i>Three-dimensional Whole Body Human Model</i>	40
<i>Two-dimensional Human Head-Neck Model</i>	42
REFERENCES.....	45

CHAPTER 1

OVERVIEW

1.1 INTRODUCTION

This report documents the progresses on developing a human biomechanical modeling toolbox during the first phase of the research project. It is separated into two parts. This first part consists of an overview of the toolbox, rigid body formulations, and example models and applications. A separate second part provides detailed description of individual routines in the toolbox.

This first part is divided into five chapters. The first chapter gives an overview of the current state of the analysis, modeling and simulation of human biomechanical system. The strategy and plan for developing a toolbox is also given. Chapter two gives the formulations for kinematics calculation with an emphasis on three-dimensional rotational kinematics. Chapter three develops forward dynamics formulations for multibody systems that are suitable for forward dynamic simulation of human systems. Chapter four describes the topics commonly associated to the inverse dynamic analysis of human biomechanical systems. Chapter five provides some example models and applications of the current version of the toolbox.

1.2 BIOMECHANICAL ANALYSIS, MODELING AND SIMULATION

1.2.1 Need for Biomechanical Modeling

The analysis, modeling and simulation of human system have become a more and more important research area. This is driven by our intrinsic curiosity of understanding the fundamental mechanisms as well as by the needs from both the civil and the military. For the military, it always faces the challenge of evaluating and improving soldiers' performance under various environmental and operational conditions, as well as reducing associated injuries. Biomechanical researchers in the military have to deal with issues such as developing better equipment to enhance soldiers' performance, design better training schedule to increase soldiers' strength without incurring injury, designing better ways of monitoring, assessing and improving the medical status of warfighters during training and combats. A very important part of these research issues is the analysis of mechanical loads and energetic requirements of the human body during various movements.

Traditionally, most biomechanical research involves only experimentation where the statistics of laboratory measurements and/or field observations is the primary research result. The experimental approach, however, suffers several limitations. First, human body is a complex, highly

nonlinear system. Significant variations of the measurements of human responses are expected, especially among different individuals. And in many cases the data cannot be repeatable with good accuracy. Therefore, the applicability of many experiment results has to be examined with caution. Second, even when statistically significant relationships can be established from experiments, the underlying mechanisms are usually too complex to be revealed. Therefore, most experiment results can only be used to answer specific questions. They usually do not provide insight into the problems themselves. Third, experimental work are often expensive and difficult to control, taking into account that a large number of people over a long period of time are usually required to get statistically significant results. Finally in many cases it is ethically impossible to perform experiments on human beings, especially when injuries may be involved in the tests.

While experimental work still remains and will always be an important part of biomechanical research, more and more efforts are being put into the use of modeling and simulation in solving biomechanical problems associated with human systems. In modeling, the human system is represented by sets of mathematical relationships including some modeling parameters. By varying model parameters, numerical simulation can be performed. Compared with experimental work, numerical simulations are usually faster, cheaper and easier to control. The models can be used for various situations and the results are more insightful.

Whether a model can be successfully used for a practical biomechanical problem depends on how accurate the model imitates the real problem, whether there are enough mathematical tools and computational power to implement the model, and whether there are enough experimental data to verify the model results. A combination of experimentation, biomechanical analysis and biomechanical modeling and simulation is usually the best approach to tackle complex real world problems. The following sections will brief summarize the current status of biomechanical analysis, modeling and simulation of human movement.

1.2.2 Model Sub-systems

Human as a living biomechanical system is a complex and integrated neural-muscular-skeletal system combining motion generation components, adaptive control, reflexes, self-analysis and learning (Barnes, Oggero et al. 1997). Any voluntary human movements are complex motions characterized by the presence of the so-called controlling and compensating parts as the result of the coordination of neural control, muscle activation, and skeletal motion generation. The central neural system sets the goal to be achieved. The neuromuscular system correspondingly control the pattern of the muscle activation generate tension. The muscle forces drive the skeletal system to generate or adjust the motion.

In modeling, the different levels of the human biomechanical system are represented by different levels of mathematical systems.

Mechanical Sub-system

Rigid body representation of the human skeletal system is commonly used where rigid bodies with masses are connected at articulations. The governing equation of motions can be obtained from the Newton-Euler formulations, Lagrange formulations or Kane's method. The resulted sets of equations include kinematic data (velocities and accelerations), kinetic data (forces and moments) and inertial properties of body segments (mass and moment of inertia).

Deformable bodies are have also been used in some models. For example, long bones can be represented as deformable beams. Finite element models and other models based on continuum mechanics are also used to model the mechanical subsystem. Simulation of specific structures, such as the foot, benefits from the use of deformable body representation, but due to the limitations of modeling complexity, rigid body formulation are mostly used in biomechanical analysis.

Actuator Sub-system

Muscles, which are the only actuators that can generate forces, are modeled by actuator subsystem governed by muscle dynamics and muscle metabolics. The formulations for the actuator subsystem include models of various complexities. Some involves only the passive elements and no active actuators are present. More sophisticated muscle models involve both the passive and the active elements. They also include the muscle insertion points in order to determine the lines of action of the muscle forces. These components obviously become highly integrated with the geometry selected for the physical representation of the body segments. The difficulties in implementing these models include the modeling of multiarticular muscles that span over more than one joint and the redundancies presented by the multiple muscles on single joints. Even more complicated models of individual muscles have also been postulated to understand muscle function. Individual muscle spindles and even individual motor units and their recruitment and neuromuscular phenomena have been modeled. However, currently, these models only serve to provide insight into how exactly muscles function.

Control Sub-system

The control subsystem with a variety of control schemes simulates the function of the neural system. Control strategies of various level of complexity have been developed. The simplest strategy is to have no actuators to control. Among controlled models, open-looped control and closed-loop control has been studied extensively. More adaptive approaches using neural network and feed forward control are also under intensive research.

1.2.3 Types of Biomechanical Analysis and Modeling

Depends on the goal of a specific biomechanical problem, various types of analysis and modeling techniques can be adopted.

Inverse Dynamics Approach

Inverse dynamics approach involves the mechanical subsystem and possibly the actuator subsystem. At the mechanical level, it calculates the joint forces and moments from segmental inertial properties, measured kinematics data and external forces.

The necessary kinematic data can be measured from accelerometers mounted on body segments. The acceleration data is then integrated to get the required velocities and displacements. More frequently, displacement data are obtained from a motion capture system (video-based or optoelectronic). The displacement data are then differentiated to obtain the velocities and accelerations.

Inertia properties of body segments can be obtained through direct measurement on the subject. There are also regression equations based on a number of anthropometric measurements such as body weight, stature and specific geometric dimensions of individual segments.

The external forces in the biomechanical analysis of human systems are usually ground reaction forces. Force plates can measure the ground reaction forces. The measured ground reaction forces usually have to be processed (filtered, synchronized with kinematics data) before can be used for inverse dynamics analysis.

At the mechanical level, the inverse dynamics analysis provides the joint forces and moments. Some energetics quantities such as internal work, external work, joint power flow may also be obtained. These kinetics and energetics quantities are used in many researches to serve the purposes such as analyzing both the healthy and pathological gait, assisting in the diagnosis of the underlying pathologies of abnormal gait pattern, helping the evaluation and design of soldier equipment, *etc.* In many of these researches, statistics analysis of test results; characterization and pattern analysis of the time history of the results have to be used.

After the joint forces and moments are obtained, they can be used to estimate muscle forces and joint reaction forces from passive structures (ligaments, tendon). Since a large number of muscles spanning each joint in the human body, the estimation of muscle forces is an indeterminate problem (Collins 1995). Techniques to solve this problem are based on either grouping muscles with similar function thus eliminating redundancy or applying optimization criteria to solve the muscle force distribution (Crowninshield 1978; Hardt 1978; Patriarco, Mann et al. 1981; Vaughan, Hay et al. 1982; Cholewicki and McGill 1994). The first approach leads to oversimplification and unsatisfactory results. The second approach is usually called inverse optimization or static optimization. The inverse optimization are numerical efficient and has been successfully applied but it also suffers from certain drawbacks. First the optimization criteria has not been completely understood. Second, the inverse optimization cannot guarantee the continuity of the solution. Third, muscle dynamics is not reflected in inverse optimization. Recently, some work (Happee 1994) has been done to include muscle dynamics as constraints in inverse optimization, which has been shown to work well to solve complex shoulder mechanism (Happee and Van der Helm 1995). Finally the

lack of reliable validation procedures also limits the application of inverse optimization. Currently, electromyogram signals, which describe the input into the muscular system is usually recorded to see if it matches with the muscle force pattern calculated from inverse dynamics optimization.

Forward Dynamics Approach

While inverse dynamics approach tries to calculate joint forces and moments and thus muscle forces from measured kinematics data, forward dynamics approach attempts to predict the motion from neural or mechanical inputs. A forward simulation may involve all the mechanical, actuator and the control systems.

When no actuator is present, only the initial conditions are required and the simulation predicts the motion trajectories. This involves only the mechanical subsystem. The approach has been widely used in simulating some traumatic events, such as car crash where the event happen in a very short period time and the effects of neural control and muscle activities can be neglected.

As a control model, the easiest one to implement is an open-loop controller with a torque that is only a function of time. This removes all the complexities associated with computing kinematics of muscle insertion points. How the joint torque changes with respect to time depends mainly on the goal of the simulation. One way is to solve the inverse dynamic problem using data collected during an experiment in which a subject performs the same actions that the simulation is trying to reproduce. Another way to obtain the torque is to impose an optimization criterion. The use of such a simplified actuator and control model cannot compensate for external perturbations and provides no means for actively maintaining balance when equilibrium conditions are desired.

When force and torque application is also a function of position, velocity or other generalized variables in the model, the control become closed loop. Muscle and spinal level reflex is an example of closed-loop control. Simulation of higher level controls, such as cerebellum and brain, becomes more challenging. More adaptive approaches, such as neural networks and artificial intelligence techniques, can be applied to model these interactions and relate other biomechanically relevant parameters to control.

Feedforward concepts are also adopted in the control theory. A feedforward controller (brain) predicts the future motion of the controlled system (the body) and compares it to the current body position. When discrepancy is noted, appropriate corrective signals are issued. A key point of feedforward control is that it is a dynamic process and this can be adapted to explain some processes of motor learning and performance enhancement. As increasing possible perturbations have been experienced during the repetitions or training, patterned responses are learned. The feedforward control requires a very accurate and rapid motion analysis. Currently, most simulations of human system do not incorporate movement analysis capability. However, further development of feedforward concept will lead to more useful simulations.

Energetics

The energetic aspect human biomechanical system deals with the mechanical power as well as the metabolic cost associated with human movements. The metabolic cost can be separated into different terms according to their sources. The activation heat accounts for the energy used to activate muscles. The maintenance heat is used to maintenance the muscle forces. The shorting heat is related to the extra heat produced as a consequence of the shortening of muscle. The mechanical work is the product of muscle force doing work. And the dissipation of energy in passive structures also contributes to the total metabolic costs. Although research work has led to some empirical relations, the actual metabolic cost is usually determined from the measured oxygen consumption, which is related to the metabolic cost.

Different methods are available to estimate the mechanical power during human movement. Some methods calculate the power based on external work necessary to move the center of mass of a human body. However, the actual dynamics of each segment is lost in these methods. Some other methods provide the mechanical power due to the movement of each segment. These models cannot account for the synergy of muscles over a single joint. Although it is recognized that the actual mechanical work and thus the metabolic cost has to come from the muscles, currently it has not been very successful in calculating muscle power due to the difficulties in determining muscle forces.

1.3 DEVELOPING A BIOMECHANICAL MODELING TOOLBOX

Human biomechanical systems are highly non-linear systems with a high number of interconnected and interacting elements. There are multilevel and multi-loop controllers involved and the systems are characterized by highly functional adaptations. Summary of the available theoretical and experimental investigations on the human biomechanical systems convinces one that a complex system approach has to be adopted. System theory implies integral analysis of the working system instead of studying of separate phenomenon. This requires the biomechanical models be simple to use, goal oriented, reliable, complete and adaptive. The basis of this is a complex of mathematical tools that can be assembled to describe the processes in real human biomechanical systems under investigation.

On the other hand, although biomechanical problems are versatile in nature. Some basic mathematical techniques are shared. Providing a set of these mathematical tools will facilitate and standardize the solution of these complex problems without reworking on the mathematical details which is usually very time consuming and error prone.

Although a large amount of commercial and research software have been developed or used in biomechanical analysis of human systems. Most of them are targeted at solving specific classes of problems. And none of them provides such a basic set of mathematical tools. It is the object of this research project to review, collect, organize and develop these fundamental mathematical tools

serving human biomechanical analysis, modeling and simulation. A human modeling toolbox will be developed with the following features

1. Flexible and powerful: users will be provided with the fundamental and powerful tools that can be used to solve very general problems. The toolbox will be organized in such a way that models can easily be assembled for problems under investigation. The results of simulation can be visualized. Attention will also be paid on the development of standard, convenient information input and editing facilities
2. Reliable: the mathematical and numerical algorithms will be rigorously tested and well studied, thus avoiding unnecessary errors in mathematical modeling which is the major source of error in biomechanical modeling
3. Efficient: complicated models can be assembled from standardized functions. Therefore, users are spared from basic programming and can concentrate on the modeling itself. In addition, higher-level routines specifically developed for common problems will also be provided
4. Consistent: developing model in a systematic way will make the comparison of results easier. Also, benchmark data and problems will also be included in the toolbox for easy calibration of model results
5. Open: the toolbox will allow the addition of new algorithms and models. This is crucial for the fast-growing biomechanical modeling research area. The open structure of the toolbox ensures that it will become more and more powerful in real applications.
6. Easy sharing of data: data will be stored in a systematic and easily retrievable way.

In order to satisfy these requirements, the following components will be included in the toolbox

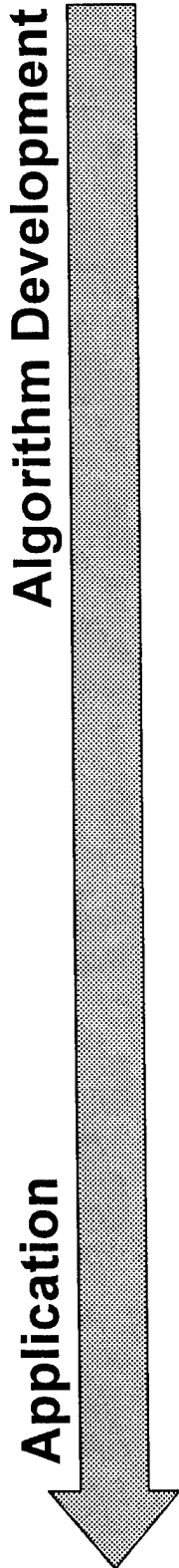
1. Rigid dynamics routines: including kinematics, inverse dynamics, and forward dynamics formulations of multibody systems with closed loop and constraints.
2. Muscle modeling routines: including various models for the passive and active elements of muscle as well as a collection of muscle parameters.
3. Control schemes and optimization routines: including inverse (static) optimization, dynamics optimization, open-looped and close-looped control using both joint torque and muscle activation as control parameters.
4. Data analysis routines: including the smoothing, fitting and filtering of time history data; statistical analysis; pattern recognition of data.
5. Graphics routines: including plotting routines for data viewing, animation routines as well as routines for developing graphic user interfaces
6. Other utility routines: including but not limited to routines for basic matrix manipulation, file input and output, data format conversion *etc.*

7. Database: including collected model parameters and simulation results as well as routines of managing the data

Matlab (Mathworks 2000) is an integrated technical environment that combines numeric computation, advanced graphics and visualization, and a high-level language. This makes it suitable for the analysis, modeling and simulation of human systems. The human modeling toolbox will be developed in Matlab. However, the use of the toolbox will not be limited in Matlab environment. Programs developed in Matlab can be compiled into standalone applications as well as web based application.

The following figure shows the schematics of the toolbox. Key to the toolbox is the lower level kernel routines that perform the above mentioned functions. Higher lever modeling routines are assembled from kernel functions for commonly encountered modeling problems. Benchmark problems will be developed based on the modeling routines. The shaded boxes in Figure 1-1, including user models and applications, are not the parts of the toolbox.

The toolbox will be developed in three phases. The first phase will focus on the rigid body formulation. The second and the third phases deal with muscle modeling and control schemes of different levels of complexity. The development of graphics and additional utility routines will spread over all the three phases.



KERNEL ROUTINES	
Rigid Dynamics Solver <ul style="list-style-type: none"> ◆ Kinematics routines ◆ Inverse dynamics routines ◆ Forward dynamics routines 	Data Analysis <ul style="list-style-type: none"> ◆ Smoothing, fitting filtering ◆ Statistics analysis ◆ Pattern recognition
Muscle dynamics <ul style="list-style-type: none"> ◆ Passive elements ◆ Active elements ◆ Muscle library 	Graphics <ul style="list-style-type: none"> ◆ 2D, 3D graphics ◆ Animation ◆ User interface tools
Control and Optimization <ul style="list-style-type: none"> ◆ Static optimization ◆ Dynamics optimization ◆ Open/close-looped control using joint torques ◆ Open/close-looped control with muscle activation ◆ Adaptive control, feed-forward control, <i>etc.</i> 	DataBase <ul style="list-style-type: none"> ◆ Model parameters ◆ Benchmark results
	Other utilities <ul style="list-style-type: none"> ◆ Basic math calculation ◆ File input/output routines ◆ Data format conversion ◆ Interface routines
MODELING ROUTINES	
<ul style="list-style-type: none"> ◆ Inverse simulation routines ◆ Forward simulation routines 	<ul style="list-style-type: none"> ◆ Data Analysis/interpretation ◆ High level graphics
BENCH MODELS	USER MODELS
<ul style="list-style-type: none"> ◆ Dynamics bench models ◆ Muscle modeling benches ◆ Control benches ◆ <i>Etc.</i> 	
APPLICATION	

Figure 1-1. Configuration of Human Biomechanical Toolbox

CHAPTER 2

MULTIBODY KINEMATICS

Kinematics is the science of motion without considering its relationship with the force applied. In human movement, it is the study of the positions, angles, velocities, and accelerations of body segments and joints during motion. Despite of the fact that many textbooks have been published on human movement (Vaughan, Davis et al. 1990; Winter 1990; Ozkaya and Nordin 1991), there is no complete and rigorous formulations for the kinematics of human movement. In addition, controversy still exists among biomechanical community on the use of different reference frames, segment orientation conventions and the definition of joint angles.

This chapter provides the background information and detailed kinematics formulations. The formulations suffice the needs for most human movement analysis. The concept of tree-structured systems and various types of coordinate frames are described. Formulations for rotational kinematics are given. Knowledge of linear algebra is required to understand the formulations. More information on kinematics are can be found in (Meirovitch 1970; Paul 1981; Kane and Levinson 1985).

2.1 TREE STRUCTURED MULTIBODY SYSTEM

A multibody system may or may not contain closed loops. When there is no closed loop in the system, it is called a tree-structured system. Systems with closed loop usually have to be converted into tree structured system by substitute parts of closed loops with kinematic constraints. A tree structured multibody system has a single rigid body called the root. The root is attached to the inertial frame through a joint. Each rigid body in the multibody structure has a unique, non-overlapping path from the root to itself.

A graph can be created from a tree-structured multibody system with the following conventions. Each rigid body is assigned as a node and each joint connecting the bodies is assigned as an edge. The inertia frame is assigned node 0. The root node is labeled with the number 1, and the remaining rigid bodies are labeled in a depth-first manner. The joints are labeled so that the joint index is the same as the unique rigid body outboard to the joint. One example of a tree-structured representation of a human of 13 bodies and 13 joints is illustrated in the following diagram.

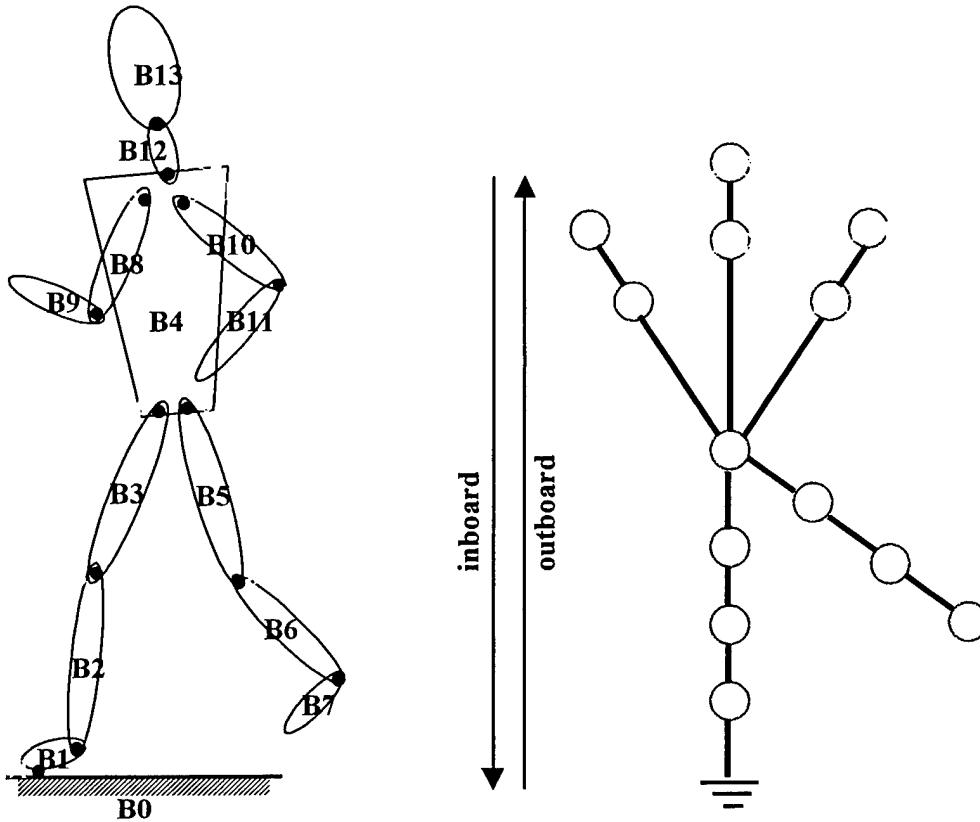


Figure 2-1. Tree-Structured Representation of a 13-segment, 13-Joint Human

Several coordinate systems, as shown in Figure 2-2, are commonly used in the analysis of a multibody system. Inertia reference system as shown in Figure 2-2(a) is usually the global coordinate system, which means the coordinates of its origin are zero and all other coordinate systems are specified with respect to this system. Each body segment has a local coordinate system (marked with subscript "L" in Figure 2-2(b), which usually has its origin at the segment mass center. The orientation of the local reference system can be arbitrary. The principal moment of inertia axes, subscripted with "P" in Figure 2-2(b), are specified with respect to the local reference system. In order to calculate joint angles, it is necessary to define two joint coordinate systems for a joint; one rigidly attached to each of the two segments that are connected by the joint, as shown in Figure 2-2(d). The orientations of the joint coordinate systems are specified by the rotation from the local reference systems of both segments. Once the two joint coordinate systems are defined, they are fixed in the corresponding segments and unable to move relative to the segments.

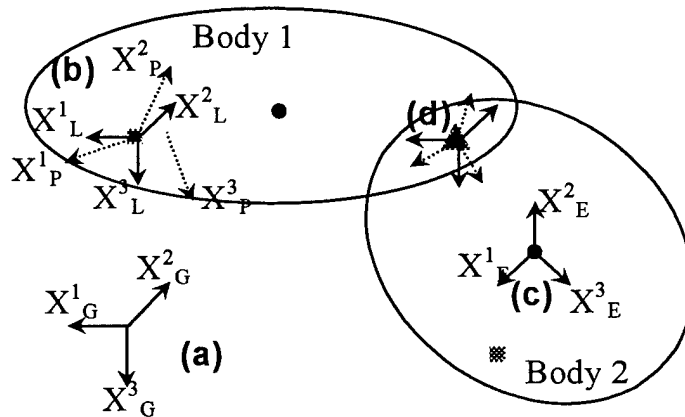


Figure 2-2. Reference coordinate systems

(a) Global coordinate system; (b) Local coordinate system and principal moment of inertia axes of segment 1 at the segment's center of mass; (c) Geometry coordinate system of segment 2 at the segment's geometric center; (d) Joint coordinate systems

The geometry of the outer surface is sometimes defined for a rigid body segment to represent the physical appearance of the segment. This is necessary for the visual representation of the body as well as used to detect contact between different rigid bodies and the environment. There is no direct association of the segment inertial properties and the shape of the contact geometry. The geometry coordinate system as shown in Figure 2-2(c) is also specified with respect to the local reference system.

2.2 REPRESENTATION OF RIGID BODY ORIENTATION

Let b_1, b_2, b_3 form the right-handed local frame of a rigid body B moving in the inertia frame A represented by a_1, a_2, a_3 ; r^B is a vector fixed in B; and r^A is the same vector expressed in A. The orientation of B with respect to A can be represented in a few ways.

2.2.1 Rotational (Orientation) Matrix

Rotational matrix is defined as the rotated frame B expressed in base frame A, *i.e.*,

$$\mathbf{R} = {}^A\mathbf{R}^B = [b_1 \ b_2 \ b_3] \quad (2.1)$$

Therefore, the invariance of vector requires the vectors expressed in A and B frames be related by the following equation

$$v^A = \mathbf{R} v^B$$

The orientation matrix is orthonormal, *i.e.*, $\mathbf{R}^T \mathbf{R} = \mathbf{I}$, where I is a unit diagonal matrix of dimension 3. This introduces six constraints and allows three independent coordinates representing the nine elements of the rotational matrix.

Also, since matrix multiplication is not commutative, special attention should be paid to the sequence of the multiplication of the rotational matrix, which indicates the frame inside which the rotation is performed.

- ◆ Post-multiplying rotational matrices ($R_A R_{B1} R_{B2} \dots$) indicates subsequently rotate with respect to rotated frame B_1, B_2 , etc.
- ◆ Pre-multiplying rotational matrices ($\dots R_{B2} R_{B1} R_A$) indicates always rotate with respect to inertia frame A.

2.2.2 Euler Angles

Definition

Rotation may also be described by three euler (cardan) angles. However, to uniquely determine the three angles, the sequence of the rotation must also be specified. ZXZ and ZYX conventions are commonly used. In ZXZ-convention, as shown in Figure 2-3(a), rotations are sequentially performed around the Z (ϕ), X (θ), and Z (ψ) axes respectively. While in ZYX-convention, as shown in Figure 2-3(b), rotations are sequentially performed around the Z (ϕ), Y (θ), and X (ψ) axes respectively.

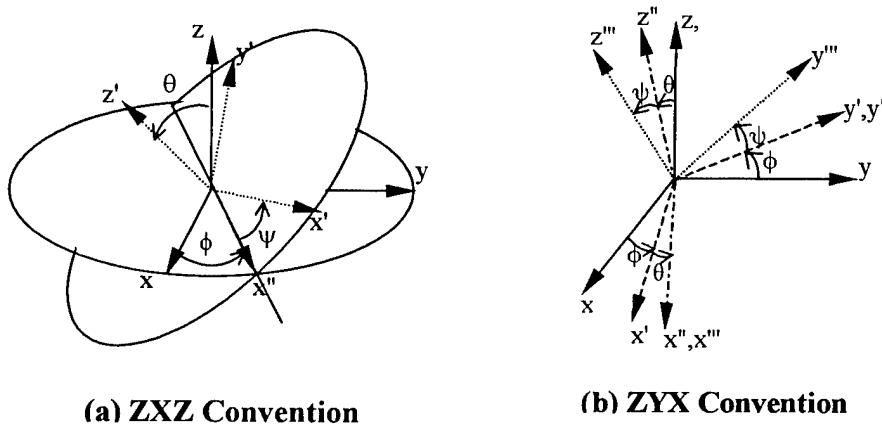


Figure 2-3. Euler Angles

Conversion between Rotational Matrix and Euler Angles

Let $c_1 = \cos(\phi)$, $s_1 = \sin(\phi)$, $c_2 = \cos(\theta)$, $s_2 = \sin(\theta)$, $c_3 = \cos(\psi)$, and $s_3 = \sin(\psi)$. Also designate R_ϕ , R_θ and R_ψ to indicate the rotational matrices around the individual axis respectively. For ZXZ convention, rotational matrix can be obtained by post-multiplying R_ϕ , R_θ , and R_ψ as

$$R_\phi = \begin{bmatrix} 1 & 0 & 0 \\ 0 & c_1 & -s_1 \\ 0 & s_1 & c_1 \end{bmatrix}; R_\theta = \begin{bmatrix} c_2 & -s_2 & 0 \\ s_2 & c_2 & 0 \\ 0 & 0 & 1 \end{bmatrix}; R_\psi = \begin{bmatrix} 1 & 0 & 0 \\ 0 & c_3 & -s_3 \\ 0 & s_3 & c_3 \end{bmatrix} \quad (2.2)$$

$$\mathbf{R} = \mathbf{R}_\phi \mathbf{R}_\theta \mathbf{R}_\psi = \begin{bmatrix} c_1 c_3 - s_1 c_2 s_3 & -c_1 s_3 - s_1 c_2 c_3 & s_1 s_2 \\ s_1 c_3 + c_1 c_2 s_3 & -s_1 s_3 + c_1 c_2 c_3 & -c_1 s_2 \\ s_2 s_3 & s_2 c_3 & c_2 \end{bmatrix} \quad (2.3)$$

For ZYX convention, the rotational matrix is

$$\mathbf{R}_\phi = \begin{bmatrix} 1 & 0 & 0 \\ 0 & c_1 & -s_1 \\ 0 & s_1 & c_1 \end{bmatrix}; \quad \mathbf{R}_\theta = \begin{bmatrix} c_2 & 0 & s_2 \\ 0 & 1 & 0 \\ -s_2 & 0 & c_2 \end{bmatrix}; \quad \mathbf{R}_\psi = \begin{bmatrix} c_2 & -s_2 & 0 \\ s_2 & c_2 & 0 \\ 0 & 0 & 1 \end{bmatrix} \quad (2.4)$$

$$\mathbf{R} = \mathbf{R}_\phi \mathbf{R}_\theta \mathbf{R}_\psi = \begin{bmatrix} c_1 c_2 & -s_1 c_3 + c_1 s_2 s_3 & s_1 s_3 + c_1 s_2 c_3 \\ s_1 c_2 & c_1 c_3 + s_1 s_2 s_3 & -c_1 s_3 + s_1 s_2 c_3 \\ -s_2 & c_2 s_3 & c_2 c_3 \end{bmatrix} \quad (2.5)$$

On the other hand, euler angles can be estimated from orientation matrix. For ZXZ convention, the algorithm is as follows

<p>when $R_{31} > \varepsilon$ or $R_{32} > \varepsilon$</p> $\begin{cases} \phi = \arctan 2(R_{13}, -R_{23}) & \phi \in [-\pi, \pi] \\ \theta = \arctan 2(s_1 R_{13} - c_1 R_{23}, R_{33}) & \theta \in [0, \pi] \\ \psi = \arctan 2(-c_1 R_{12} - s_1 R_{22}, c_1 R_{11} + s_1 R_{21}) & \psi \in [-\pi, \pi] \end{cases}$ $\begin{cases} \phi = \arctan 2(R_{13}, -R_{23}) & \phi \in [-\pi, \pi] \\ \theta = \arctan 2(s_1 R_{13} - c_1 R_{23}, R_{33}) & \theta \in [-\pi, 0] \\ \psi = \arctan 2(-c_1 R_{12} - s_1 R_{22}, c_1 R_{11} + s_1 R_{21}) & \psi \in [-\pi, \pi] \end{cases} \quad (2.6)$ <p>when $R_{31} \leq \varepsilon$ and $R_{32} \leq \varepsilon$</p> $\begin{cases} \phi = 0 \\ \theta = \arctan 2(-R_{23}, R_{33}) & \theta \in [-\pi, \pi] \\ \psi = \arctan 2(-R_{12}, R_{11}) & \psi \in [-\pi, \pi] \end{cases}$
--

where arctan2 is the extension of regular arctan function allowing the calculation of an angle from $-\pi$ to π . The first argument of the function should be the sin-component of the angle, while the second component be the cos-component of the angle.

For ZYX convention, euler angles can be calculated from rotational matrix as

$$\begin{array}{l}
\text{when } R_{31} > \varepsilon \text{ or } R_{32} > \varepsilon \\
\left\{ \begin{array}{ll} \phi = \arctan 2(R_{32}, -R_{33}) & \phi \in [-\pi, \pi] \\ \theta = \arctan 2(-R_{31}, s_3 R_{32} + c_3 R_{33}) & \theta \in [-\pi/2, \pi/2] \\ \psi = \arctan 2(s_3 R_{22} + c_3 R_{23}, s_3 R_{12} + c_3 R_{23}) & \psi \in [-\pi, \pi] \end{array} \right. \\
\left\{ \begin{array}{ll} \phi = \arctan 2(-R_{32}, R_{33}) & \phi \in [-\pi, \pi] \\ \theta = \arctan 2(-R_{31}, s_3 R_{32} + c_3 R_{33}) & \theta \in [-\pi, -\pi/2] \text{ and } \theta \in [\pi/2, \pi] \\ \psi = \arctan 2(s_3 R_{22} + c_3 R_{23}, s_3 R_{12} + c_3 R_{23}) & \psi \in [-\pi, \pi] \end{array} \right. \\
\text{when } R_{31} \leq \varepsilon \text{ and } R_{32} \leq \varepsilon \\
\left\{ \begin{array}{ll} \phi = 0 & \\ \theta = \arctan 2(-R_{31}, R_{33}) & \theta \in [-\pi, \pi] \\ \psi = \arctan 2(R_{23}, R_{13}) & \psi \in [-\pi, \pi] \end{array} \right.
\end{array} \quad (2.7)$$

It should be noted that using euler angles doesn't limit the range of the orientation angles, thus can handle tumbling motions. However, using rotational matrix cannot by itself account for the tumbling motion. On the other hand, Euler angles suffers from the so-called "gimbal locking", when two of the three rotational axes coincide and the derivatives of the euler angles are indeterminate.

2.2.3 Euler Parameters

Definition

In order to avoid the locking of euler angles, rotation can be represented by quaternion which uses four coordinates rather than three. The basic idea of the quaternion representation of rotation is that any rotation can be uniquely defined as a rotation (β) around a unit vector (λ). The euler parameters, defined as follows, is one of the many quaternions

$$\left\{ \begin{array}{l} e_1 = \lambda_1 \sin\left(\frac{\beta}{2}\right) \\ e_2 = \lambda_2 \sin\left(\frac{\beta}{2}\right) \\ e_3 = \lambda_3 \sin\left(\frac{\beta}{2}\right) \\ e_4 = \cos\left(\frac{\beta}{2}\right) \end{array} \right. \quad (2.8)$$

Notice since λ is a unit vector, the norm of euler parameters $[e_1, e_2, e_3, e_4]^T$ is one. As can be seen from the definition, the tumbling motion cannot be accounted for by using euler parameters

Conversion between Rotational Matrix and Euler Parameters

Rotational matrix can be calculated from euler parameters as

$$\mathbf{R} = \begin{bmatrix} 1 - 2(e_2^2 + e_3^2) & 2(e_1e_2 - e_3e_4) & 2(e_1e_3 + e_2e_4) \\ 2(e_1e_2 + e_3e_4) & 1 - 2(e_1^2 + e_3^2) & 2(e_2e_3 - e_1e_4) \\ 2(e_1e_3 - e_2e_4) & 2(e_2e_3 + e_1e_4) & 1 - 2(e_1^2 + e_2^2) \end{bmatrix} \quad (2.9)$$

Euler parameters can be determined from a given rotational matrix by the following scheme

```

if trace(R)+1>0
    e=norm {
        R32 - R23
        R13 - R31
        R21 - R12
        1.0 + trace(R)
    }
else
    i = 1; j = 2; k = 3 (default)
    i = 2; j = 3; k = 1 (R22 > R11)
    i = 3; j = 1; k = 2 (R33 > Rii)
    ei = 1.0 - trace(R)+2.0Rii
    ej = Rij + Rji
    ek = Rik + Rki
    e4 = Rkj - Rjk
    e = norm(e)
end

```

(2.10)

2.3 ANGULAR VELOCITY AND ACCELERATION

The angular velocity of a rigid body B ($\mathbf{b}_1, \mathbf{b}_2, \mathbf{b}_3$) moving in the inertia frame A ($\mathbf{a}_1, \mathbf{a}_2, \mathbf{a}_3$) is defined as follows

$${}^A\boldsymbol{\omega}^B = \mathbf{b}_1 \frac{d}{dt} \mathbf{b}_2 \cdot \mathbf{b}_3 + \mathbf{b}_2 \frac{d}{dt} \mathbf{b}_3 \cdot \mathbf{b}_1 + \mathbf{b}_3 \frac{d}{dt} \mathbf{b}_1 \cdot \mathbf{b}_2 \quad (2.11)$$

Angular acceleration is defined as the time derivative of the angular acceleration

$${}^A\boldsymbol{\alpha}^B = \frac{d}{dt} {}^A\boldsymbol{\omega}^B \quad (2.12)$$

Relationship between angular velocity of a rigid body, ${}^A\boldsymbol{\omega}^B$, and the time derivatives of euler angles, $\dot{\boldsymbol{\phi}} = [\dot{\phi} \dot{\theta} \dot{\psi}]^T$, can be determined from the invariance of the angular velocity vector with respect to the reference frame. For ZXZ convention, it is

$${}^A\omega^B = \mathbf{S}\dot{\phi} = \begin{bmatrix} s_2s_3 & c_3 & 0 \\ s_2c_3 & -s_3 & 0 \\ c_2 & 0 & 1 \end{bmatrix} \begin{Bmatrix} \dot{\phi} \\ \dot{\theta} \\ \dot{\psi} \end{Bmatrix} \quad (2.13)$$

For ZYX convention the relationship is

$${}^A\omega^B = \mathbf{S}\dot{\phi} = \begin{bmatrix} -s_2 & 0 & 1 \\ c_2s_3 & c_3 & 0 \\ c_2c_3 & -s_3 & 0 \end{bmatrix} \begin{Bmatrix} \dot{\phi} \\ \dot{\theta} \\ \dot{\psi} \end{Bmatrix} \quad (2.14)$$

The inverse relationship is

$$\dot{\phi} = \mathbf{T}^A\omega^B = \mathbf{S}^{-1}{}^A\omega^B \quad (2.15)$$

It must be noticed that the T matrix (the inverse of S matrix) may be singular in certain cases. Physically, the singular case corresponds to the "locking" of euler angles, when angular velocity can not be determined from euler angles.

Similarly, the time derivatives of euler parameters can be calculated from segment angular velocity from the following equation

$$\dot{\mathbf{e}} = \begin{Bmatrix} \dot{e}_1 \\ \dot{e}_2 \\ \dot{e}_3 \\ \dot{e}_4 \end{Bmatrix} = \mathbf{T}^A\omega^B = \frac{1}{2} \begin{bmatrix} e_4 & -e_3 & e_2 \\ e_3 & e_4 & -e_1 \\ -e_2 & e_1 & e_4 \\ -e_1 & -e_2 & -e_3 \end{bmatrix} {}^A\omega^B \quad (2.16)$$

2.4 TRACKING TUMBLING MOTION

The formulations given above are capable of handling translation between the different representations of rotation, *i.e.*, rotational matrix, euler angles or euler parameters. However, they are not exactly the same. Euler angles allow for the tumbling motion (where rotation is not limited to one cycle), but they suffer from the problem of "locking". Euler parameters have no problem with locking, but cannot handle tumbling motion naturally.

In calculation angular velocity, the time derivatives of either euler angles or Euler parameters must be obtained. Therefore their continuity in time must be considered. To simplify the problem, rotation is represented by a rotational matrix. Euler angles are estimated from rotational matrix, which further will be differentiated and used to calculate angular velocity. As can be seen from equations (2.6) and (2.7), The range ϕ and θ are limited to 2π (one circle), while the range of ψ is limited to π (half a circle). To guarantee the continuity of Euler angles, two extensions to the formulations must be made. First, the range of θ has to be extended to the full circle. Equations (2.6) and (2.7) give two set of formulations to calculate Euler angles corresponding to cases when θ is inside different half circles. Using formulations for one half cycle, sudden jumps of π or $-\pi$ in the

values of ϕ and ψ indicates that θ has moved to the other half circle. Second, jumps of 2π in Euler angles have to be removed. This requires the time history of the rotation be recorded.

2.5 LINEAR POSITION, VELOCITY AND ACCELERATION

Six independent parameters are required to describe a local frame $B(\mathbf{b}_1, \mathbf{b}_2, \mathbf{b}_3)$ with respect to the inertial frame $A(\mathbf{a}_1, \mathbf{a}_2, \mathbf{a}_3)$, i.e., three independent parameters describing the orientation of B , as described in the previous sections, and three coordinates of the origin of B expressed in A . Let O^B the origin of local frame B ; \mathbf{p}^B the position vector of a fixed point on B ; and \mathbf{p}^A the same position vector expressed in A . The following relationship holds

$$\mathbf{p}^A = {}^A R^B \mathbf{p}^B + O^B \quad (2.17)$$

The velocity, \mathbf{v}^A , and the acceleration, \mathbf{a}^A , of the point expressed in the inertia frame are defined as

$$\mathbf{v}^A \triangleq \frac{d}{dt} \mathbf{p}^A \quad (2.18)$$

$$\mathbf{a}^A \triangleq \frac{d}{dt} \mathbf{v}^A \quad (2.19)$$

The following equations relate the velocities and the accelerations expressed in A and B frames

$$\mathbf{v}^A = \mathbf{v}^B + {}^A \boldsymbol{\omega}^B \times \mathbf{r}^B \quad (2.20)$$

$$\mathbf{a}^A = \mathbf{a}^B + {}^A \boldsymbol{\omega}^B \times ({}^A \boldsymbol{\omega}^B \times \mathbf{r}^B) + {}^A \boldsymbol{\alpha}^B \times \mathbf{r}^B \quad (2.21)$$

where ${}^A \boldsymbol{\omega}^B$ and ${}^A \boldsymbol{\alpha}^B$ are the angular velocities and accelerations of the local B frame.

2.6 CONSTRAINTS

The motion of a multibody system may involve two types of constraints. Configuration constraints restrict the positions of each rigid body. The equations expressing the restriction are called holonomic constraint equations. Motion constraints impose restrictions on the velocities of the rigid bodies. When there is no motion constraint involved in a multibody system, it is called a holonomic system; otherwise, it is a nonholonomic system. The first and second order partial derivatives of rotational matrix, R , with respect to euler angles or euler parameters must be provided for the formulations of a holonomic system. The first order partial derivatives of T matrix are also needed for the nonholonomic systems. These relationships are given in the following tables.

Table 2-1 1st order derivative of R with respect to ZXZ euler angles

	$\partial/\partial\phi$	$\partial/\partial\theta$	$\partial/\partial\psi$
R_{11}	$-s_1 s_3 - c_1 c_2 c_3$	$s_1 s_2 s_3$	$-c_1 s_2 - s_1 c_2 c_3$
R_{21}	$c_1 c_3 - s_1 c_2 s_3$	$-c_1 s_2 s_3$	$-s_1 s_3 + c_1 c_2 c_3$
R_{31}	0	$c_2 s_3$	$s_2 c_3$

R_{12}	$s_3 - c_1 c_2 c_3$	$s_1 s_2 c_3$	$-c_1 c_3 + s_1 c_2 s_3$
R_{22}	$-c_1 s_3 - s_1 c_2 c_3$	$-c_1 s_2 c_3$	$-s_1 c_3 - c_1 c_2 s_3$
R_{23}	0	$c_2 c_3$	$-s_2 s_3$
R_{31}	$c_1 s_2$	$s_1 c_2$	0
R_{32}	$s_1 s_2$	$-c_1 c_2$	0
R_{33}	0	$-s_2$	0

Table 2-2 2nd order derivative of R with respect to ZXZ euler angles

	$\partial^2/\partial\phi^2$	$\partial^2/\partial\theta^2$	$\partial^2/\partial\psi^2$	$\partial^2/\partial\phi\partial\theta$	$\partial^2/\partial\phi\partial\psi$	$\partial^2/\partial\theta\partial\psi$
R_{11}	$-c_1c_3 + s_1c_2s_3$	$s_1c_2s_3$	$-c_1c_3 + s_1c_2s_3$	$c_1s_2s_3$	$s_1s_3 - c_1c_2c_3$	$s_1s_2c_3$
R_{21}	$-s_1c_3 - c_1c_2s_3$	$-c_1c_2s_3$	$-s_1c_3 - c_1c_2s_3$	$s_1s_2s_3$	$-c_1s_3 - s_1c_2c_3$	$-c_1s_2c_3$
R_{31}	0	$-s_2s_3$	$-s_2s_3$	0	0	c_2c_3
R_{12}	$c_1s_3 + s_1c_2c_3$	$s_1c_2c_3$	$c_1s_3 + s_1c_2c_3$	$c_1s_2c_3$	$s_1c_3 + c_1c_2s_3$	$-s_1s_2s_3$
R_{22}	$s_1s_3 - c_1c_2c_3$	$-c_1c_2c_3$	$s_1s_3 - c_1c_2c_3$	$s_1s_2c_3$	$-c_1c_3 + s_1c_2s_3$	$c_1s_2s_3$
R_{23}	0	$-s_2s_3$	$-s_2s_3$	0	0	$-c_2s_3$
R_{31}	$-s_1s_2$	$-s_1s_2$	0	c_1c_2	0	0
R_{32}	c_1s_2	c_1s_2	0	s_1c_2	0	0
R_{33}	0	$-c_2$	0	0	0	0

Table 2-3 1st order derivative of R with respect to ZYZ euler angles

	$\partial/\partial\phi$	$\partial/\partial\theta$	$\partial/\partial\psi$
R_{11}	$-s_1c_2$	$-c_1s_2$	0
R_{21}	c_1c_2	$-s_1s_2$	0
R_{31}	0	$-c_2$	0
R_{12}	$-c_1c_3 - s_1s_2s_3$	$c_1c_2s_3$	$s_1s_3 + c_1s_2c_3$
R_{22}	$-s_1c_3 + c_1s_2s_3$	$s_1c_2s_3$	$-c_1s_3 + s_1s_2c_3$
R_{23}	0	s_2s_3	c_2c_3
R_{31}	$c_1s_3 - s_1s_2c_3$	$c_1c_2c_3$	$s_1c_3 - c_1s_2s_3$
R_{32}	$s_1s_3 + c_1s_2c_3$	$s_1c_2c_3$	$-c_1c_3 - s_1s_2s_3$
R_{33}	0	$-s_2c_3$	c_2s_3

Table 2-4 2nd order derivative of R with respect to ZYZ euler angles

	$\mathcal{F}/\partial\phi^2$	$\mathcal{F}/\partial\theta^2$	$\mathcal{F}/\partial\psi^2$	$\mathcal{F}/\partial\phi\partial\theta$	$\mathcal{F}/\partial\phi\partial\psi$	$\mathcal{F}/\partial\theta\partial\psi$
R_{11}	$-c_1c_2$	c_1c_2	0	s_1s_2	0	0
R_{21}	$-s_1c_2$	$-s_1c_2$	0	$-c_1s_2$	0	0
R_{31}	0	s_2	0	0	0	0
R_{12}	$s_1c_3 - c_1s_2s_3$	$-c_1s_2s_3$	$s_1c_3 - c_1s_2s_3$	$-s_1c_2s_3$	$c_1s_3 - s_1s_2c_3$	$c_1c_2c_3$
R_{22}	$-c_1c_3 - s_1s_2s_3$	$-s_1s_2s_3$	$-c_1c_3 - s_1s_2s_3$	$c_1c_2s_3$	$s_1s_3 + c_1s_2c_3$	$s_1c_2c_3$
R_{23}	0	$-c_2s_3$	$-c_2s_3$	0	0	$-s_2c_3$
R_{31}	$-s_1s_2 - c_1s_2c_3$	$-c_1s_2c_3$	$-s_1s_2 - c_1s_2c_3$	$-s_1c_2c_3$	$c_1c_3 + s_1s_2s_3$	$-c_1c_2s_3$
R_{32}	$c_1s_3 - s_1s_2c_3$	$-s_1s_2c_3$	$c_1s_3 - s_1s_2c_3$	$c_1c_2c_3$	$s_1c_3 - c_1s_2s_3$	$-s_1c_2s_3$
R_{33}	0	c_2c_3	$-c_2c_3$	0	0	s_2s_3

Table 2-5 Derivatives of T with respect to ZXZ Euler Angles

	$s_2 > \epsilon$			$s_2 < \epsilon$
	$\partial/\partial\phi$	$\partial/\partial\theta$	$\partial/\partial\psi$	
T_{11}	0	$-c_2s_3/s_2^2$	c_3/s_2	Locking
T_{21}	0	0	$-s_3$	
T_{31}	0	s_3/s_2^2	$-c_2c_3/s_2^2$	
T_{12}	0	$-c_2c_3/s_2^2$	$-s_3/s_2$	
T_{22}	0	0	$-c_3$	
T_{23}	0	$-c_3/s_2^2$	c_2s_3/s_2	
T_{31}	0	0	0	
T_{32}	0	0	0	
T_{33}	0	0	0	

Table 2-6 Derivatives of T with respect to ZYX Euler Angles

	$s_2 > \epsilon$			$s_2 < \epsilon$
	$\partial/\partial\phi$	$\partial/\partial\theta$	$\partial/\partial\psi$	Locking
T_{11}	0	0	0	
T_{21}	0	0	0	
T_{31}	0	0	0	
T_{12}	0	$s_2 s_3 / c_2^2$	c_3 / c_2	
T_{22}	0	0	$-s_3$	
T_{23}	0	s_3 / c_2^2	$s_2 c_3 / c_2$	
T_{31}	0	$s_2 c_3 / c_2^2$	s_3 / c_2	
T_{32}	0	0	$-c_3 -c_3$	
T_{33}	0	c_3 / c_2^2	$-s_2 s_3 / c_2$	

Table 2-7 1st order derivative of R with respect to euler parameters

	$\partial/\partial e_1$	$\partial/\partial e_2$	$\partial/\partial e_3$	$\partial/\partial e_4$
R_{11}	0	$-4e_2$	$-4e_3$	0
R_{21}	$2e_2$	$2e_1$	$2e_4$	$2e_3$
R_{31}	$2e_3$	$-2e_4$	$2e_1$	$-2e_2$
R_{12}	$2e_2$	$2e_1$	$-2e_4$	$-2e_3$
R_{22}	$-4e_1$	0	$-4e_3$	0
R_{23}	$2e_4$	$2e_3$	$2e_2$	$2e_1$
R_{31}	$2e_3$	$2e_4$	$2e_1$	$2e_2$
R_{32}	$-2e_4$	$2e_3$	$2e_2$	$-2e_1$
R_{33}	$-4e_1$	$-4e_2$	0	0

Table 2-8 2nd order derivative of R with respect to euler parameters

	$\partial/\partial e_1^2$	$\partial/\partial e_2^2$	$\partial/\partial e_3^2$	$\partial/\partial e_4^2$	$\partial/\partial e_1 \partial e_2$	$\partial/\partial e_1 \partial e_3$	$\partial/\partial e_1 \partial e_4$	$\partial/\partial e_2 \partial e_3$	$\partial/\partial e_2 \partial e_4$	$\partial/\partial e_3 \partial e_4$
R_{11}	0	-4	-4	0	0	0	0	0	0	0
R_{21}	0	0	0	0	2	0	0	0	0	2
R_{31}	0	0	0	0	0	2	0	0	-2	0
R_{12}	0	0	0	0	2	0	0	0	0	-2
R_{22}	-4	0	-4	0	0	0	0	0	0	0
R_{23}	0	0	0	0	0	0	2	2	0	0
R_{31}	0	0	0	0	0	2	0	0	2	0
R_{32}	0	0	0	0	0	0	-2	2	0	0
R_{33}	-4	-4	0	0	0	0	0	0	0	0

Table 2-9 Derivative of T with respect to euler parameters

	$\partial/\partial e_1$	$\partial/\partial e_2$	$\partial/\partial e_3$	$\partial/\partial e_4$
T_{11}	0	0	0	0.5
T_{21}	0	0	0.5	0
T_{31}	0	-0.5	0	0
T_{41}	-0.5	0	0	0
T_{12}	0	0	-0.5	0
T_{22}	0	0	0	0.5
T_{32}	0.5	0	0	0
T_{42}	0	-0.5	0	0
T_{13}	0	0.5	0	0
T_{23}	-0.5	0	0	0
T_{33}	0	0	0	0.5
T_{43}	0	0	-0.5	0

CHAPTER 3

FORWARD DYNAMICS FORMULATION

In human motion simulation, human body is assumed to be a multibody constrained system of rigid segments connected at certain joints. There are a few ways of formulating the system. The traditional approach has been to select a set of minimal coordinates and formulate the equations of motion as a second-order system of ordinary differential equations (ODE). The ODEs are then integrated by standard ODE solvers (Meirovitch 1970; Kane and Levinson 1985). However, recently effort has been made to formulate the system in descriptor form, which use non-minimal sets of coordinates (Lubich, Engstler et al. 1995). Descriptor formulation leads to a set of differential algebraic equations (DAE) including equations of motion (second order ODEs) and constraint equations (differential or algebraic equations).

This chapter develops a numerical method to solve the resultant DAEs from descriptor formulation by converting the algebraic equations into differential equations. The relaxation of position and velocity constraints is compensated in the method by projecting the integration results back to the original constraint manifolds. This method can solve both open-looped and close-looped systems.

3.1 GOVERNING EQUATION

The equations of motion of a constrained articulate system can be expressed in terms of position vector $\mathbf{p}(t)$, velocity vector $\mathbf{v}(t)$ and Lagrange multipliers $\lambda(t)$ as

$$\begin{aligned} \text{(a)} \quad & \dot{\mathbf{p}} = \mathbf{T}(t, \mathbf{p})\mathbf{v} \\ \text{(b)} \quad & \mathbf{M}\dot{\mathbf{v}} = \mathbf{f}(t, \mathbf{p}, \mathbf{v}, \lambda) - \mathbf{T}(\mathbf{p})^T \mathbf{G}(t, \mathbf{p})^T \lambda \\ \text{(c)} \quad & \mathbf{g}(t, \mathbf{p}) = \mathbf{0} \end{aligned} \tag{4.1}$$

with prescribed initial conditions

$$\mathbf{p}(t_0) = \mathbf{p}_0, \mathbf{v}(t_0) = \mathbf{v}_0 \tag{4.2}$$

In equation (4.1), (a) relates the time derivative of position to the velocity; (b) indicates the conservation of momentum; and (c) represents the position constraints. \mathbf{G} is the derivative of the constraints with respect to position variables, *i.e.*,

$$\mathbf{G}(t, \mathbf{p}) = \frac{\partial \mathbf{g}}{\partial \mathbf{p}}$$

Let n_p , n_v and n_λ denote the number of position variables, the number of velocity variables and the number of Lagrange multipliers respectively. The interpretation and dimension of the variables in equation (4.1) is summarized in Table 3-1.

Table 3-1. Definition and dimension of variables

Variable	Definition	Dimension
p	Position	\mathbb{R}^{n_p}
v	Velocity	\mathbb{R}^{n_v}
λ	Lagrange multipliers	\mathbb{R}^{n_λ}
g	Constraint	\mathbb{R}^{n_λ}
f	External force	\mathbb{R}^{n_v}
M	Mass matrix	$\mathbb{R}^{n_v \times n_v}$
T	Velocity description matrix	$\mathbb{R}^{n_p \times n_v}$
G	$\partial \mathbf{g} / \partial \mathbf{p}$	$\mathbb{R}^{n_\lambda \times n_p}$

The algebraic constraint equation in (4.1) has to be converted into ordinary differential equations. Differentiation of the (c) of equation (4.1) with respect to time leads to the following equation

$$\boxed{\frac{dg_i}{dt} = g_{i,t} + g_{i,j} \dot{p}_j = 0} \quad (4.3)$$

where index notation is used and subscript $,t = \partial / \partial t$ indicates partial differentiation of time and subscript $,j = \partial / \partial p_j$ indicates partial differentiation of the j^{th} component of the position vector. Equation (4.3) replaces the position constraints by the equivalent velocity constraints.

Differentiating (4.3) again with respect to time leads to

$$\frac{d^2 g_i}{dt^2} = g_{i,tt} + g_{i,tj} \dot{p}_j + (g_{i,j})_t \dot{p}_j + g_{i,j} (\dot{p}_j)_t = 0$$

Notice $\dot{p}_j = T_{ij} v_j$ and $T_{ij,t} = 0$, equation (4.3) can be rewritten as

$$g_{i,j} T_{jk} \dot{v}_k = -\{g_{i,tt} + 2g_{i,tj} \dot{p}_j + g_{i,jk} \dot{p}_j \dot{p}_k + g_{i,j} T_{jk,l} \dot{p}_l v_k\} \quad (4.4)$$

Equation (4.4) replaces the position constraints by acceleration constraints. Therefore, the ODE formulation of the constrained articulated system takes the following form

$$\boxed{\begin{aligned} \text{(a)} \quad & \dot{\mathbf{p}} = \mathbf{T}(t, \mathbf{p}) \mathbf{v} \\ \text{(b)} \quad & \mathbf{M} \dot{\mathbf{v}} = \mathbf{f}(t, \mathbf{p}, \mathbf{v}, \boldsymbol{\lambda}) - \mathbf{T}(\mathbf{p})^T \mathbf{G}(t, \mathbf{p})^T \boldsymbol{\lambda} \\ \text{(c)} \quad & \mathbf{G}(t, \mathbf{p}) \mathbf{T}(\mathbf{p}) \dot{\mathbf{v}} = -(\mathbf{g}^t + \mathbf{g}^a + \mathbf{g}^b) \end{aligned}} \quad (4.5)$$

with $\mathbf{g}^t = g_{i,tt} + 2g_{i,tj} \dot{p}_j$; $\mathbf{g}^a = g_{i,jk} \dot{p}_j \dot{p}_k$; and $\mathbf{g}^b = g_{i,j} T_{jk,l} \dot{p}_l v_k$
and $\mathbf{p}(t_0) = \mathbf{p}_0, \mathbf{v}(t_0) = \mathbf{v}_0$

3.2 NUMERICAL FORMULATION

\mathbf{M} is a n_v by n_v square matrix. When formulated in natural coordinate system, \mathbf{M} is also block diagonal and positive definite. Therefore, (b) of equation (4.5) can be rewritten as

$$\dot{\mathbf{v}} = \mathbf{M}^{-1} \{ \mathbf{f} - \mathbf{T}^T \mathbf{G}^T \boldsymbol{\lambda} \}$$

By substituting it into (c), the explicit form of $\boldsymbol{\lambda}$ is obtained as

$$\boldsymbol{\lambda} = (\mathbf{GTM}^{-1}\mathbf{T}^T\mathbf{G}^T)^{-1} \{ \mathbf{GTM}^{-1}\mathbf{f} + \mathbf{g}^t + \mathbf{g}^a + \mathbf{g}^b \}$$

Notice that $\mathbf{GTM}^{-1}\mathbf{T}^T\mathbf{G}^T$ is always a positive definite square matrix. Therefore, the following standard system of first-order equations is obtained

$$\begin{aligned} \mathbf{y} &= \begin{Bmatrix} \mathbf{p} \\ \mathbf{v} \end{Bmatrix} \\ \dot{\mathbf{y}} &= \begin{Bmatrix} \dot{\mathbf{p}} \\ \dot{\mathbf{v}} \end{Bmatrix} \\ \dot{\mathbf{p}} &= \mathbf{T}\mathbf{v} \\ \dot{\mathbf{v}} &= \mathbf{M}^{-1} \left\{ \mathbf{f} - \mathbf{T}^T \mathbf{G}^T (\mathbf{GTM}^{-1}\mathbf{T}^T\mathbf{G}^T)^{-1} (\mathbf{GTM}^{-1}\mathbf{f} + \mathbf{g}^t + \mathbf{g}^a + \mathbf{g}^b) \right\} \end{aligned} \quad (4.6)$$

Equation (4.6) can be solved using the ODE solvers in Matlab.

3.3 PROJECTION OF POSITION AND VELOCITY CONSTRAINTS

Equation (4.5) and its numerical counterpart equation (4.6), the position constraints (the (c) of equation (4.1)) are replaced by the acceleration constraints. During numerical integration, numerical drifting may occur and the position constraints and velocity constraints (4.3) may not be accurately satisfied. The projection method (Lubich, Engstler et al. 1995) is used to project the solution to the position and velocity constraint manifolds. The projection equations are given as follows.

3.3.1 Projection of position constraint

After a successful integration step, an approximate position solution \mathbf{p}^0 is obtained. It is projected to the position constraint $\mathbf{g}(t, \mathbf{p}) = \mathbf{0}$ by performing the following Newton-Raphson iterations

$$\begin{aligned} \begin{bmatrix} \mathbf{M}(\mathbf{p}^0) & \mathbf{T}(\mathbf{p}^0)^T \mathbf{G}(\mathbf{p}^0)^T \\ \mathbf{G}(\mathbf{p}^0) \mathbf{T}(\mathbf{p}^0) & \mathbf{0} \end{bmatrix} \begin{Bmatrix} \Delta\boldsymbol{\gamma}^k \\ \boldsymbol{\mu}^{k+1} \end{Bmatrix} &= - \begin{Bmatrix} \mathbf{M}(\mathbf{p}^0) \boldsymbol{\gamma}^k \\ \mathbf{g}(t, \mathbf{p}^k) \end{Bmatrix} \\ \boldsymbol{\gamma}^{k+1} &= \boldsymbol{\gamma}^k + \Delta\boldsymbol{\gamma}^k \\ \mathbf{p}^{k+1} &= \mathbf{p}^k + \mathbf{T}(\mathbf{p}^0) \Delta\boldsymbol{\gamma}^k \end{aligned} \quad (4.7)$$

until $\|\mathbf{T}(\mathbf{p}^0)\Delta\gamma^k\| \leq \text{tolerance}$.

3.3.2 Projection of velocity constraint

Velocity constraint (4.3) can also be written in matrix form as $\mathbf{g}^i + \mathbf{G}\mathbf{v} = 0$. After a successful integration step, an approximate velocity solution \mathbf{v}^0 is obtained. The velocity constraint is implemented by the following projection

$$\boxed{\begin{bmatrix} \mathbf{M}(\mathbf{p}^0) & \mathbf{T}(\mathbf{p}^0)^T \mathbf{G}(\mathbf{p}^0)^T \\ \mathbf{G}(\mathbf{p}^0)\mathbf{T}(\mathbf{p}^0) & \mathbf{0} \end{bmatrix} \begin{Bmatrix} \mathbf{v} \\ \boldsymbol{\mu} \end{Bmatrix} = \begin{Bmatrix} \mathbf{M}(\mathbf{p}^0)\mathbf{v}^0 \\ -\mathbf{g}^i \end{Bmatrix}} \quad (4.8)$$

CHAPTER 4

INVERSE DYNAMICS ANALYSIS

When human body is assumed to be a system of rigid segments connected at certain joints, human motion is governed by a set of equations of motion which include body segment parameters, driving forces and moments, and kinematic data. In the previous chapter, the equations are solved for the kinematics given the body segment parameters and the driving forces. The equations can also be solved for driving forces given the body segment parameters and the kinematics. This is called inverse dynamics approach.

Inverse dynamics approach is commonly used in biomechanical analysis of human motion to estimate the mechanical loads on joint and segments. Besides rigid body assumption, it is also assumed that no translational movement can occur at joint. The joint forces and moments calculated from inverse dynamics analysis are the resultant forces or moments from active skeletal muscles and passive joint structures such as ligaments and joint capsules. The calculated forces and moments can be further processed to yield muscle forces as well as some energetics quantities such as internal work, external work, and joint power flow. These kinetics, energetics and muscle quantities can be used to analyze both the healthy and pathological gait, assist in the diagnosis of the underlying pathologies of abnormal gait pattern, and help the evaluation and design of soldier equipment. This chapter describes some common issues of inverse dynamics analysis.

4.1 MEASURING KINEMATIC DATA AND GROUND REACTION FORCE

The kinematic data required for inverse dynamic analysis include the positions, velocities and accelerations of segment centers of gravity (CG) and rotational angles, angular velocities and angular accelerations of all segments. The displacements of body segments can be measured from a motion capture system. The displacements are then differentiated to derive the velocities and accelerations of the segments. Goniometers and accelerometers can be used to complement the estimation from the motion capture system (Ladin and Wu 1991; van den Bogert, Read et al. 1996).

Ground reaction forces can be measured by force plates, foot contact pressure measurement devices (Han, Paik et al. 1999) or alternately estimated from the kinematic data (Bobbert, Schamhardt et al. 1991). The kinematic data and the ground reaction data must be synchronized.

4.2 KINEMATICS RECONSTRUCTION

A video based motion capture system records the positions of clusters of markers attached on the surfaces of body segments in the global (laboratory) reference system. The recorded coordinates

are used to reconstruct the positions of anatomical landmarks (joint positions) and the orientation of the segments and thus the positions of segment centers of gravity.

At least three markers are needed for each segment. Given the position of three non-collinear markers on a segment and assume that there is no relative movement between the markers, the joint position can easily be reconstructed. The orientation of the segment can be calculated by geometric rules. Both the distance between the markers associated with each marker and the offset of each marker from the line connecting any other two should be sufficiently large to prevent excessive error propagation during reconstruction. However since the markers are placed on the surfaces of segments, relative movement of markers (skin marker artifacts) may exist. It has been shown that the errors in kinematic reconstruction due the skin marker artifacts can be overwhelming (Cappozzo, Cappello et al. 1997).

In order to remove the effects of the skin movement artifacts, a few techniques have been developed by putting more markers on each segment. The redundancy of the marker data allows for an optimal identification by using either a singular value decomposition algorithm or a weighted least square algorithm (Spoor and Veldpaus 1980; Veldpaus, Woltring et al. 1988; Soderkvist and Wedin 1993).

4.3 BODY SEGMENT PARAMETERS

The body segment parameters refer to the inertial parameters of a body segment, such as the mass of the segment, its length, the location of its center of gravity with respect to the segment local coordinate frame and moments of inertia (the values and orientation of the principal moments of inertia). The accuracy of the body segment parameters affects the accuracy in the kinetic analysis (Krabbe, Farkas et al. 1997).

A number of ways have been used to estimate the body segment parameters. The inertia properties can be measured directly from cadavers (Dempster 1955; Chandler, Clauser et al. 1975). However, these data include only limited sample size, age and morphological discrepancy. Mass and density of individual segments can also be determined from direct measurements on living subjects. A number of techniques such as magnetic resonance imaging (Martin, Mungiole et al. 1989; Mungiole and Martin 1990) and computerized tomography (Brooks and Jacobs 1975; Huang and Wu 1976; Zatsiorsky and Seluyanov 1985) have been used. These techniques can provide very accurate *in vivo* estimates of the segmental inertial properties. However, these techniques are difficult to perform due to exposure to radiation, high cost and lengthy procedure. Also, the direct measurement of inertial properties can not satisfy the need in assessing all the body segment parameters on individual subjects. Therefore, many linear and nonlinear statistical regression equations are developed based on the measured data (Hinrichs 1985; Yeadon and Morlock 1989; Vaughan, Davis et al. 1990; Zatsiorsky, Seluyanov et al. 1990). In addition, body segment parameters can be calculated mathematically using the assumption that the segment can be represented by simple geometry with uniform density (Jensen 1978; Hatze 1980; Jensen 1989). High

accuracy has been reported and an automated version is developed based on video image capturing and computer image processing (Sarfaty and Ladin 1993).

4.4 JOINT DYNAMICS FORMULATION

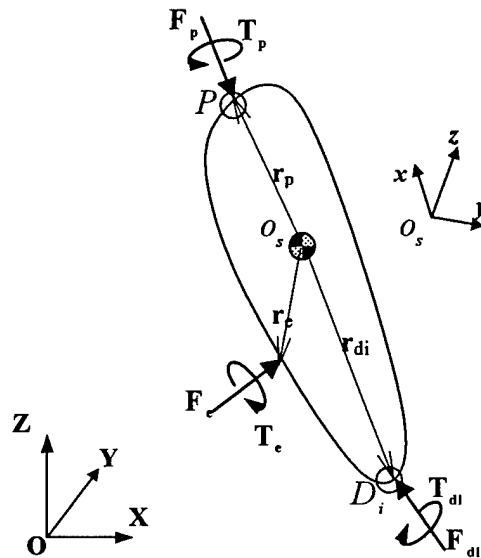


Figure 4-1 Free diagram of a segment

Figure 4-1 shows the free diagram of a segment with global frame, segment local frame, external forces and joint reaction forces displayed. Coordinate system $O(X, Y, Z)$ is the global reference frame. Local coordinate system is defined at the segment center of gravity o_s as $o_s(x, y, z)$. Therefore, orientation of the segment can be represented by the rotational matrix $R^s = {}^O R^o = [x \ y \ z]$. Points P and D_i are the proximal and distal joints of the segment. Subscript i indicates more than one distal joints may be present on one segment (say, two hip joints as distal joints of trunk segment). However, only one proximal joint is allowed.

At the proximal joint, reaction force vector F_p and reaction torque vector T_p have positive poles, which means the positive direction of the force or torque components is the same as the positive direction of the corresponding local coordinate. While at the distal joint(s), reaction force vector F_{di} and reaction torque vector T_{di} have negative poles. Vectors r_p and r_{di} represent the relative positions of the proximal and distal joints respectively. Force vector F_e is the additional external force acting on the segment. Several or none F_e may be involved depending on the situation. Similarly, vector T_e stands for the external torque exerted on the segment by the environment. One example of the external force is the ground reaction forces acting on ankles. Vector r_e shows the relative position of the application point of external force to o_s .

Let m_s indicate the mass of the segment; I_s the inertia matrix of the segment as described in the previous section; and g the gravity vector. Let a_s , ω_s and α_s be the linear acceleration vector,

angular velocity vector and angular acceleration vector of the segment, represented in the global frame, respectively. The equation of motion can be obtained by conservation of momentum as follows

$$\mathbf{F}_e + \mathbf{F}_p - \sum \mathbf{F}_{di} = m_s \mathbf{a}_s \quad (4.1)$$

$$\mathbf{T}_e + \mathbf{T}_p + \mathbf{r}_p \times \mathbf{T}_e - \sum \mathbf{r}_{di} \times \mathbf{T}_{di} = \mathbf{I}_s \cdot \boldsymbol{\alpha}_s + \boldsymbol{\omega}_s \times (\mathbf{I}_s \cdot \boldsymbol{\omega}_s) \quad (4.2)$$

Since kinematic data \mathbf{a}_s , $\boldsymbol{\omega}_s$ and $\boldsymbol{\alpha}_s$ are obtained from kinematic reconstruction and the differentiation of the position data, equations (4.1) and (4.2) for each segment can be solved by starting with the most distal segment and proceeding to the most proximal one.

The resultant joint reaction forces and torques calculated from equations (4.1) and (4.2) are defined in global reference coordinate system, which are usually not suitable for interpreting relative to the subject's joints. Therefore, the joint forces and torques are usually transformed to a body fixed anatomical reference frame. The anatomical coordinate system first proposed by [Grood, 1983 #1] is widely used [Apkarian, 1989 #5; Chen, 1988 #4; Siegler, 1988 #3; Vaughan, 1990 #6]. Also, it should be noticed that the calculated joint loads are the resultant loads from active muscles as well as the passive structures.

CHAPTER 5

EXAMPLES AND APPLICATIONS

This chapter gives sample applications and example models developed from AHBM V 1. Among inverse dynamic applications, Gait3D V1, a three-dimensional gait analysis program is developed for USARIEM; a new method is developed for a DOT project to understand the airbag external load behavior and bag-occupant interaction; and a three-dimensional lower extremity benchmark model is developed. Among forward dynamic examples, a simple spring mass model and a double pendulum model are developed to test the kinematics and integration algorithms of the toolbox. A three-dimensional whole body human model and a two-dimensional human head-neck model are developed for impact simulations.

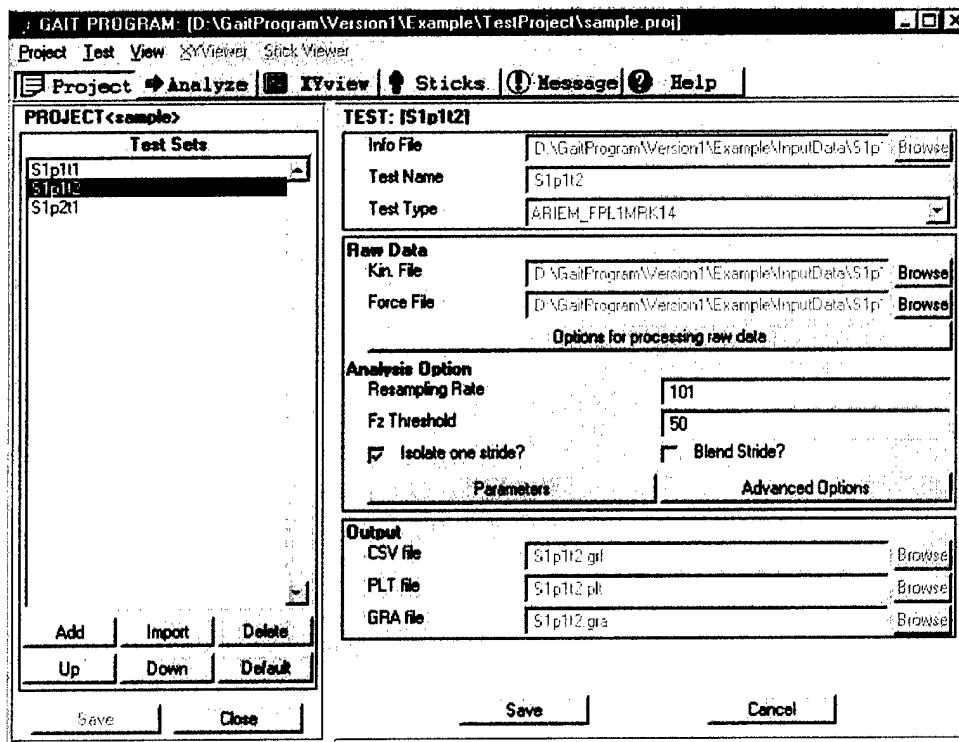
5.1 INVERSE DYNAMICS EXAMPLES AND APPLICATIONS

5.1.1 Gait3D V1 Developed for USAREIM

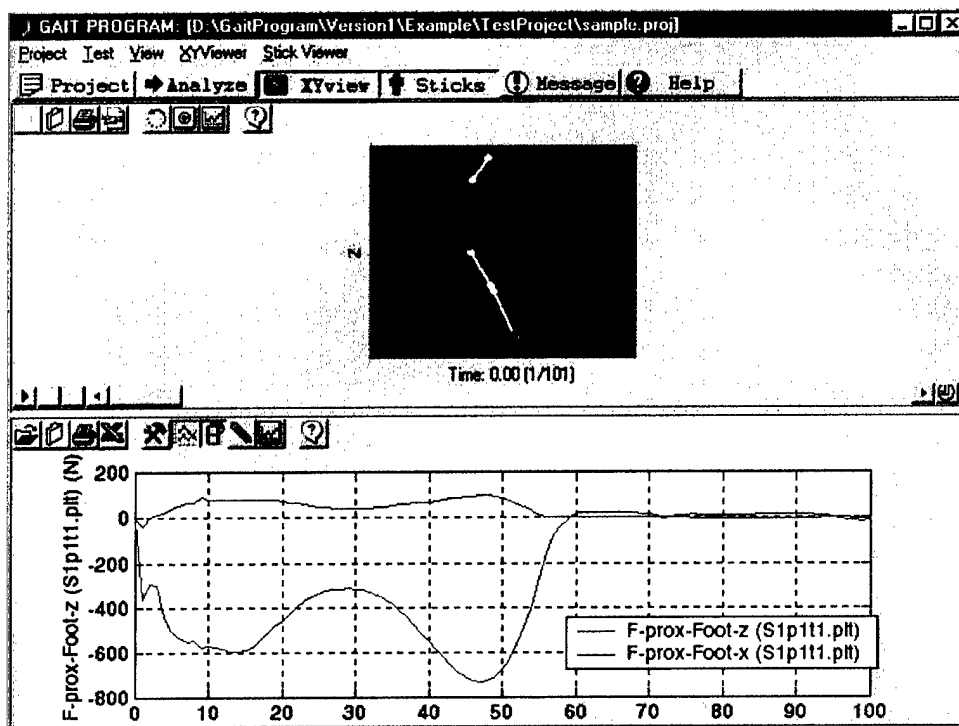
The kinematics, inverse dynamics and graphical algorithms of the AHBM toolbox are used to develop a three-dimensional gait analysis program for the U.S. Army Research Institute of Environmental Medicine (USARIEM). The version-1 of the program, Gait3D V1 (Shen 2000), supports the current test setup of USARIEM motion analysis system. Input and output file formats currently used by USARIEM are fully supported.

Gait3D V1 allows running, visualizing and analyzing multiple gait tests in a simple graphical layout. It supports running multiple tests in one project and provides easy control of analysis parameters. Gait3D V1 also comes with the StickViewer and XYviewer developed in the AHBM toolbox. These viewers allow the visualization and animation of test results.

If requested by USARIEM, the program will be upgraded to include the further development of AHBM toolbox in the following phases.



(a) Graphical Layout to Edit Multiple Gait Tests



(b) StickerViewer and XYViewer

Figure 5-1. Gait3D V1 Developed for USARIEM

5.1.2 Inverse Dynamics Model for Predicting Airbag Forces

An inverse model as shown in Figure 5-2, is developed for calculating external air bag loads on the head and neck of a small female test dummy using recorded dummy response data (Chan, Shen et al. 2001). This work is sponsored by Department of Transportation to understand and minimize the possible hazard of air bags based on physical principles.

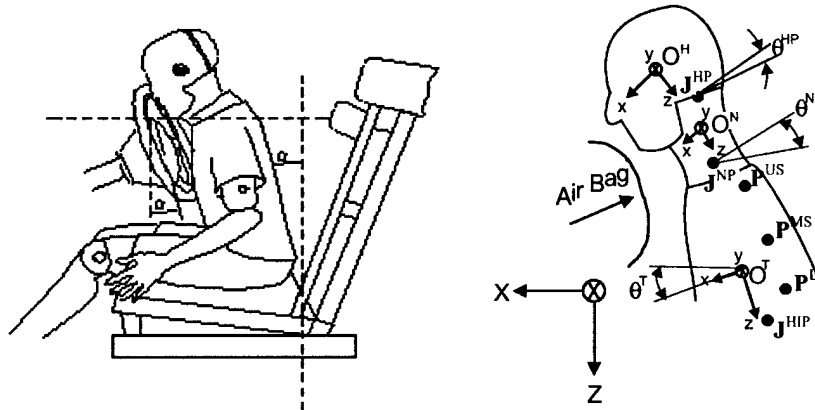
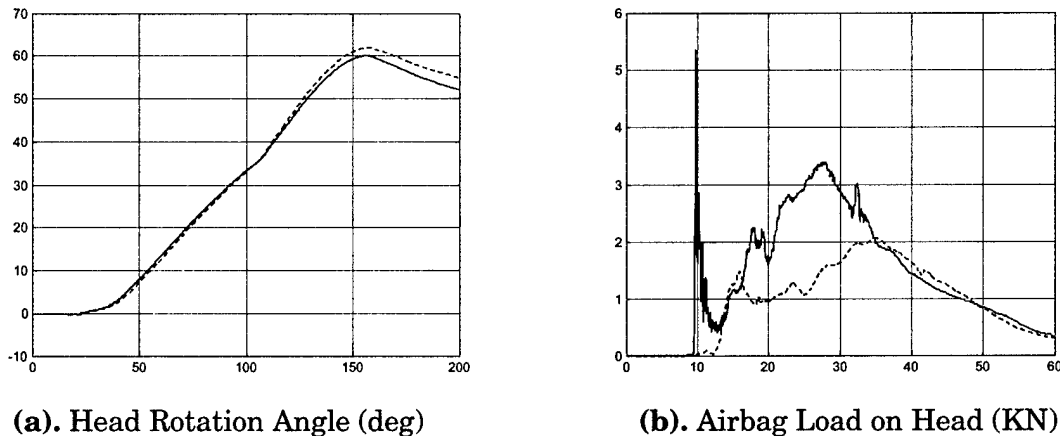


Figure 5-2. Schematics of the Inverse Model to Predict Airbag Force

Calculations are performed for static out-of-position tests as well as vehicle crash tests. Some sample calculations are given in Figure 5-3. The calculated external loads provide a phenomenological explanation of the differences in dummy responses between different dummy positions. It is also shown that the impact angle on the head affects the head/neck joint load significantly.



(a). Head Rotation Angle (deg)

(b). Airbag Load on Head (KN)

Figure 5-3. Calculated Head Rotation and Airbag Load

5.1.3 A three-dimensional lower extremity model

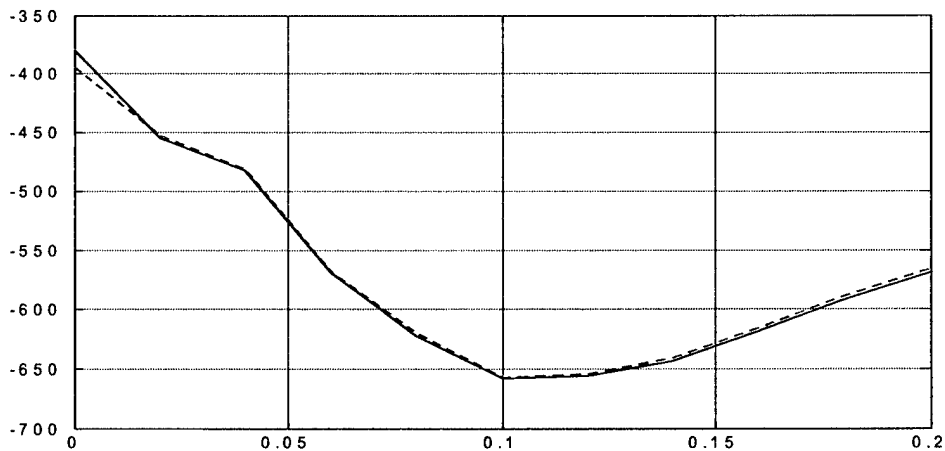
A three-dimensional lower extremity model (Vaughan, Davis et al. 1990) is developed. This model consists of seven segments, i.e., feet, shanks, thighs and a pelvis. Six joints, ankles, knees and hips, connect the seven segments. In the bench problem described in (Vaughan, Davis et al. 1990), the three-dimensional motion (positions and orientations) of the lower extremity is reconstructed from eighteen markers attached to the segments. Two force plates record the ground reaction forces on both feet. The mass and inertia properties of each segment are calculated from regression equations.



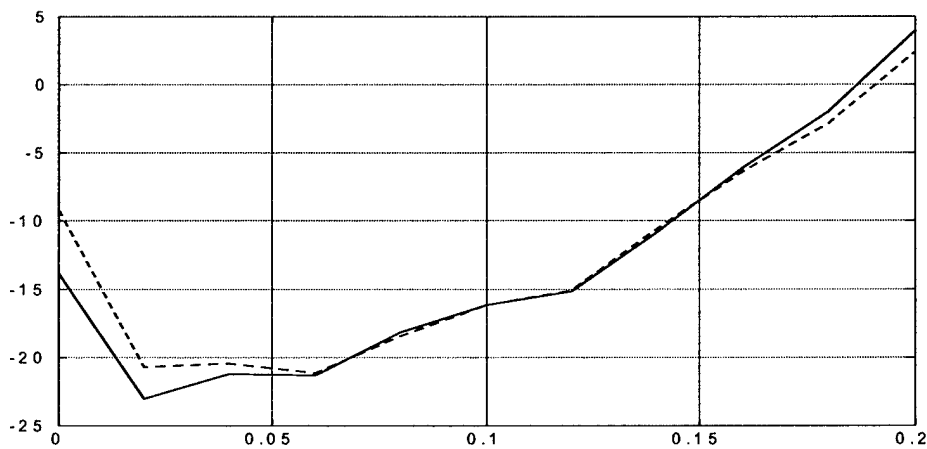
Figure 5-4. A three-dimensional lower extremity model

The kinematics and ground reaction forces given in (Vaughan, Davis et al. 1990) are used to test the kinematic and inverse dynamic routines in the toolbox. Results are consistent to those given in the book. Some of the comparison of result is given in Figure 5-5.

This model can be used to perform three-dimensional gait analysis. Lower extremity muscles will be added to the model in the next phase of AHBM development. This will allow the comparison and testing of different muscle models and muscle functions during human locomotion.



(a) Proximal/distal force at the right ankle joint in Newton. Red line is the result calculated using toolbox routines; blue line is from (Vaughan, Davis et al. 1990)



(b) Flexion/Extension torque at the right ankle joint in (Nm). Red line is the result calculated using toolbox routines; blue line is from (Vaughan, Davis et al. 1990)

Figure 5-5. Comparison of Forces and Torques at the Right ankle

5.2 FORWARD DYNAMICS ANALYSIS EXAMPLES

5.2.1 Simple Spring Mass Model

Figure 5-6 shows a simple model where two masses, m_1 and m_2 , are connect by a linear spring with a spring coefficient of k . A time dependent force $F(t)$ is applied on mass m_1 . This problem is used to test the numerical algorithm in the toolbox to solve equations of motion. Figure 5-7(b)-(d) give the solution under a cyclic load $F(t) = 10\sin(2*\pi *t)$ (Figure 5-7(a)) and $m_1 = 10$ (kg); $m_2 = 10$ (kg); $k = 10$ (N/m).

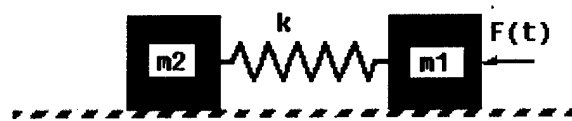
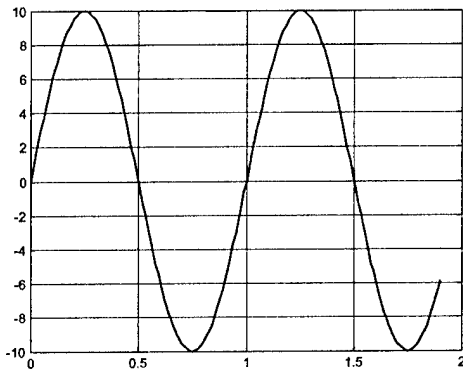
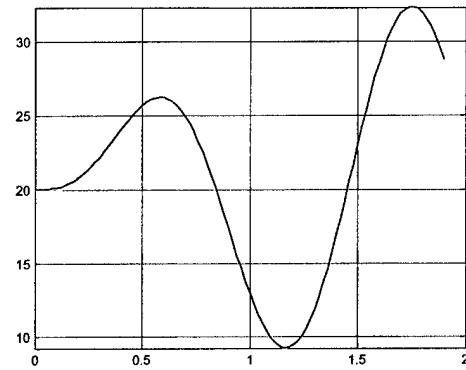


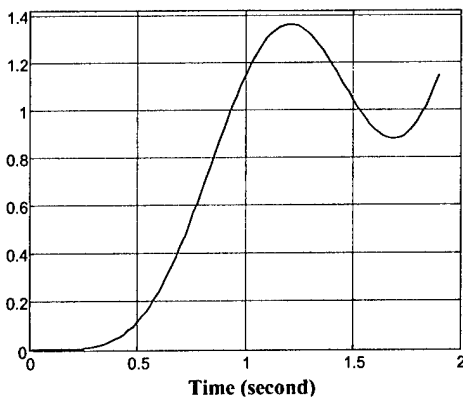
Figure 5-6. A mass-spring-mass system



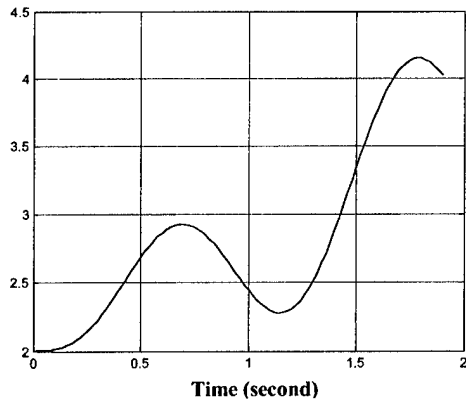
(a). External Force



(b). Spring reaction force



(c). Position of Mass #1



(d). Position of Mass #2

Figure 5-7. External force and solutions

5.2.2 Three-dimensional Double Pendulums

A three-dimensional double pendulum is shown in Figure 5-8. The lower pendulum is connected to the ground by a pin joint, where rotation is allowed around only one axis of the joint. An Euler joint connects the upper and the lower pendulum and allows for subsequent rotation around all three axes of the joint. This problem is used to test the algorithms in the toolbox to calculate three-dimensional kinematics.

In this example, both pendulums are of unit lengths, unit masses and unit moments of inertia. A constant unit force is applied at the top of the upper pendulum and moves with the pendulum (expressed in the upper pendulum local frame). The calculated kinematics is given in Figure 5-9(a)-(d).

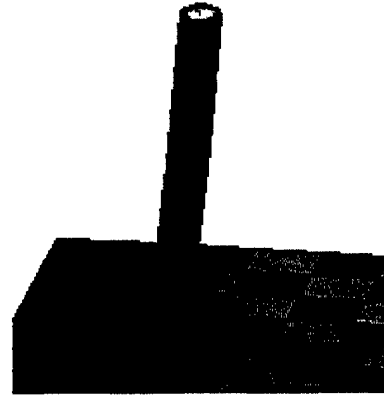
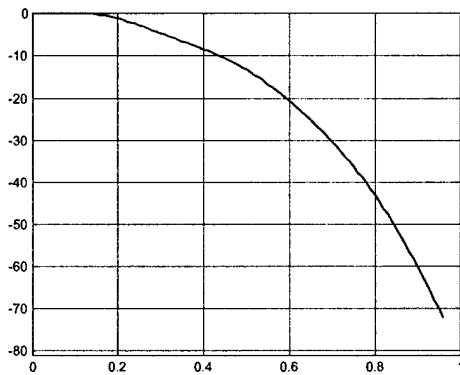
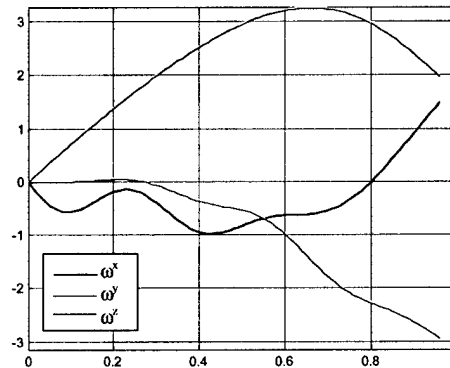


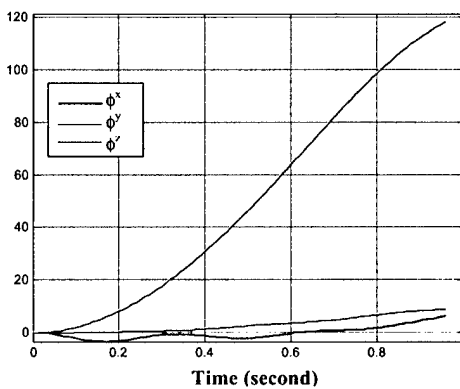
Figure 5-8. 3D Double Pendulum



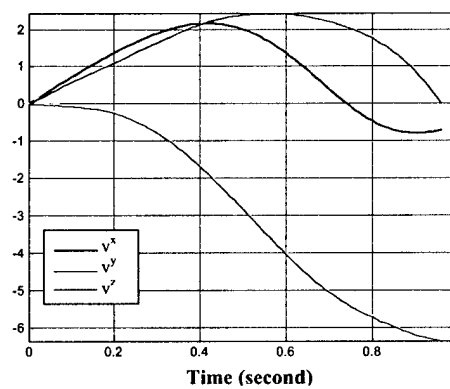
(a) Lower (pin) joint angle (deg)



(b) Upper pendulum ang. vel. (rad/s)



(c) Upper (Euler) joint angles (deg)



(d) Upper pendulum vel. (m/s)

Figure 5-9. Calculated Kinematics of the Double Pendulum

5.2.3 Three-dimensional Whole Body Human Model

Figure 5-10 shows a three-dimensional whole body model developed using AHBM V1 routines. The model has 15 body segments, i.e., head, neck, upper torso (thorax), center torso (abdomen), lower torso (pelvis), upper arms, lower arms, upper legs, lower legs and feet. The lower arms are combinations of the forearms and hands. The are connected together by 14 joints representing the physical joints of the human body such as pelvis, waist, neck, hips, knees, ankles, shoulders and elbows.

Various types of joints, such as pin joint, ball and socket joint and euler joint, are used. The joints are constrained by nonlinear rotational springs and dampers. Joint range of motion is implemented by including "soft joint stop", i.e., when angles beyond the joint range of motion, a restoring torque of significant magnitude is added to move the joint back to the range of motion.

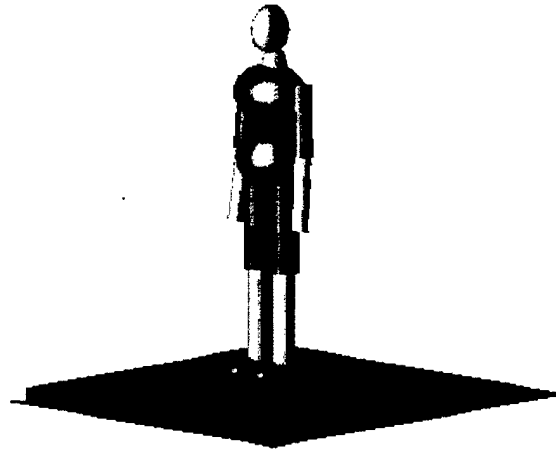
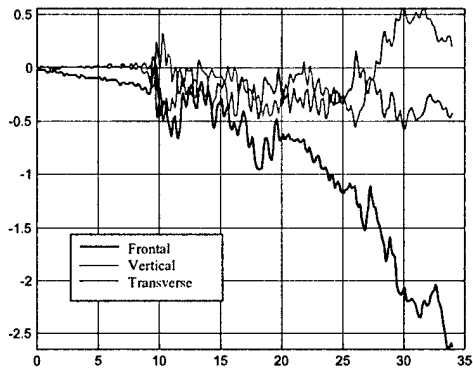


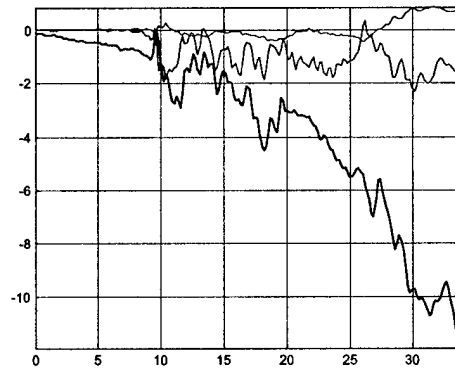
Figure 5-10. Three-dimensional 15-segment human model

The body segment inertia and geometrical properties and joint mechanical properties refer to (Cheng, Obergefell et al. 1994). These values are easily adjustable due to the flexibility of toolbox routines. The example used here has a weight of about 75 kilograms and a height of about 1.8 meters. Based on these two parameters, it is classified in the 95th percentile of the adult U.S. males

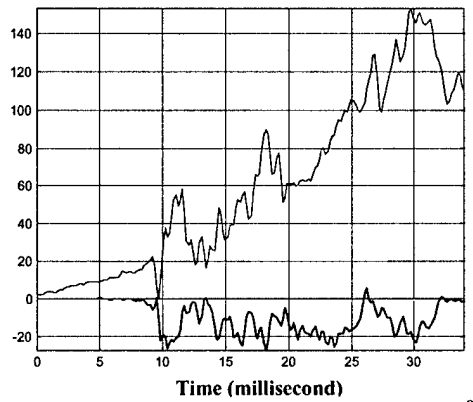
An impact force as shown in Figure 5-11(a) is applied at the chest. The model is used to calculate the response of the whole body to the impact. The chest acceleration, head acceleration and head angular accelerations are given in Figure 5-11(b)-(d).



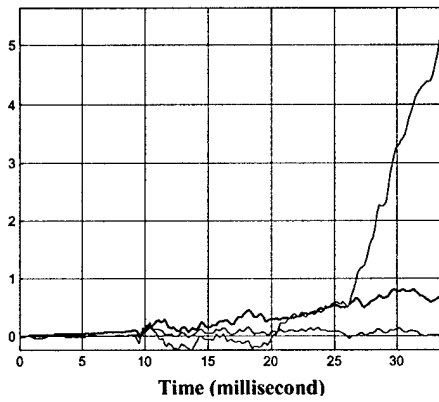
(a) Impact Force on Chest (KN)



(b) Chest Acceleration (g)



(c) Head Angular Acceleration (rad/s^2)



(d) Head Acceleration (g)

Figure 5-11. Impact Force and Calculated Accelerations

This model shows the capability of toolbox routines in dealing with impact forward simulation problems of large degrees of freedom and complex joint constraints.

5.2.4 Two-dimensional Human Head-Neck Model

A human head-neck model is developed using AHBM toolbox routines. This model is a simplified version of the global human head-neck model described by (De Jager 1996). As shown in Figure 5-12, nine rigid bodies represent the head (C0), the seven cervical vertebrae (C1-C7) and the first thoracic vertebra (T1). The inertia and geometrical properties of each segment were measured from test and given in (De Jager 1996). The bodies are connected by complex nonlinear viscoelastic elements.

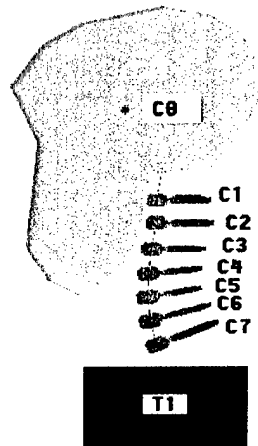
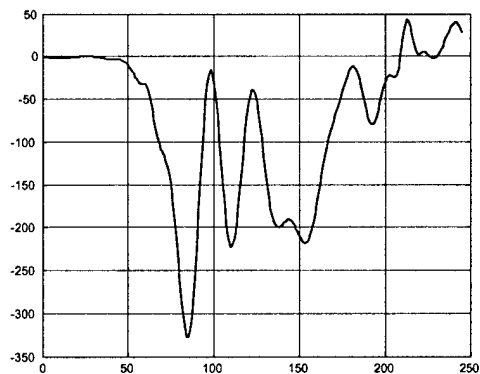


Figure 5-12. Two-dimensional Human Head Neck Model

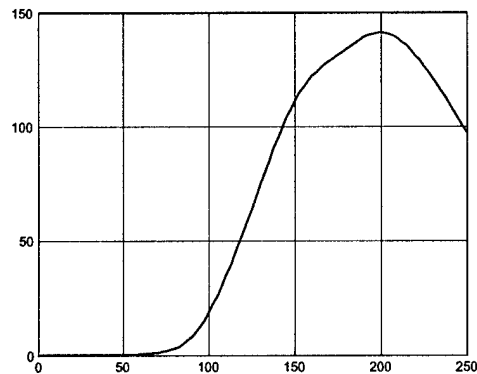
The model is used to simulate the head-neck response during a front impact test. The sled acceleration history is given in Figure 5-13(a). The simulation results are consistent with those given in (De Jager 1996). Part of the simulation results, such as total head rotation angle and joint angles between some neighboring cervical vertebra are given in Figure 5-13(b)-(f).

Since the neck joints are connected by nonlinear springs which may become very stiff at certain alignment and orientation. This model demonstrates the toolbox's ability of solving stiff problems.

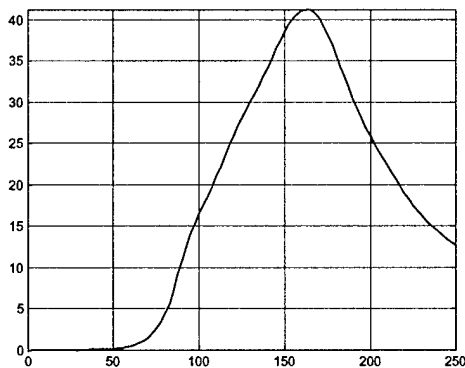
The simulation results also show that the effects of active neck muscles must be included for accurate prediction of head-neck response, even under very violent situations when the muscle effects are usually neglected.



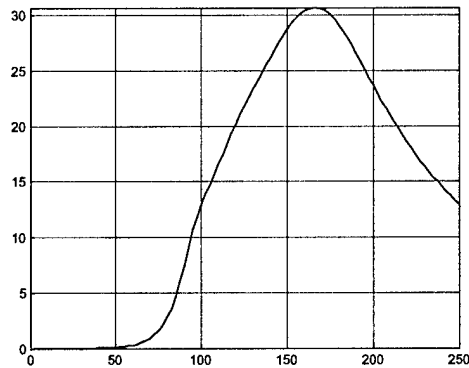
(a) Sled Acceleration (on T1) (m/s²)



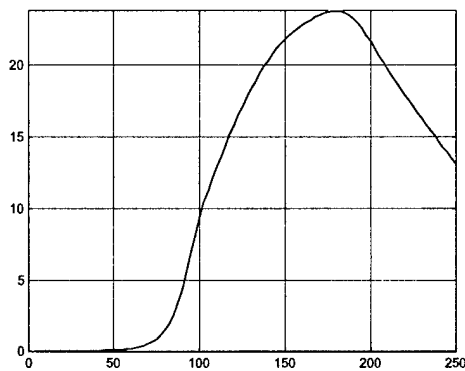
(b) Head Rotation Angle (deg)



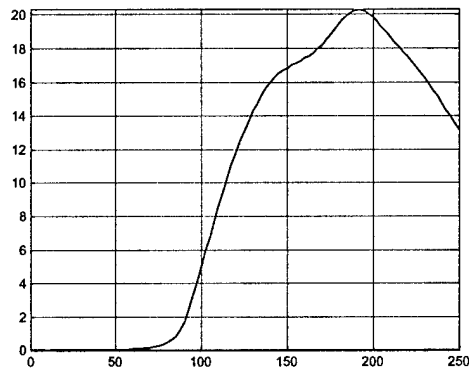
(c) Joint angle between C7-T1 (deg)



(d) Joint angle between C6-C7 (deg)



(e) Joint angle between C5-C6 (deg)



(f) Joint angle between C4-C5 (deg)

Figure 5-13. Sled Acceleration, Head and Joint Angles

REFERENCES

- Barnes, S., E. Oggero, et al., Eds. (1997). Simulation of human movement: goals, model formulation, solution techniques and considers. Three Dimensional Analysis of Human Locomotion, John Wiley and Sons, Inc.
- Bobbert, M. F., H. C. Schamhardt, et al. (1991). "Calculation of vertical ground reaction force estimates during running from positional data." J Biomech 24(12): 1095-105.
- Brooks, C. B. and A. M. Jacobs (1975). "The gamma mass scanning technique for inertial anthropometric measurement." Med Sci Sports 7(4): 290-4.
- Cappozzo, A., A. Cappello, et al. (1997). "Surface-marker cluster design criteria for 3-D bone movement reconstruction." IEEE Trans Biomed Eng 44(12): 1165-74.
- Chan, P. C., W. Shen, et al. (2001). Analysis of Air Bag Loads by Inverse Dynamics. Biomechanics Research: Experimental and Computational, Preceedings of the Twenty Seventh International Workshop.
- Chandler, R. F., C. E. Clauser, et al. (1975). Investigation of inertia propertis of the human body. Dayton, Ohio, Wright-Patterson Air Force Base.
- Cheng, H., L. A. Obergefell, et al. (1994). Generator of Body (GEBOD) Manual.
- Cholewicki, J. and S. M. McGill (1994). "EMG assisted optimization: a hybrid approach for estimating muscle forces in an indeterminate biomechanical model." J Biomech 27(10): 1287-9.
- Collins, J. J. (1995). "The redundant nature of locomotor optimization laws." J Biomech 28(3): 251-67.
- Crowninshield, R. D. (1978). "Use of Optimization Techniques to Predict Muscle Forces." J Biomech Eng Trans ASME 100: 88-92.
- De Jager, M. K. J. (1996). Mathematical head-neck models for acceleration impacts. ENGINEERING, BIOMEDICAL (0541); APPLIED MECHANICS (0346), TECHNISCHE UNIVERSITEIT EINDHOVEN (THE NETHERLANDS): 144.
- Dempster, W. T. (1955). Space requirements of seated operator: geometrical, kinematic and mechanical aspects of the body with special reference to the limbs. Dayton, Ohio, Wrighth Air Development Center, WADC.
- Han, T. R., N. J. Paik, et al. (1999). "Quantification of the path of center of pressure (COP) using an F-scan in-shoe transducer." Gait & Posture 10(3): 248-54.
- Happee, R. (1994). "Inverse dynamic optimization including muscular dynamics, a new simulation method applied to goal directed movements." J Biomech 27(7): 953-60.
- Happee, R. and F. C. Van der Helm (1995). "The control of shoulder muscles during goal directed movements, an inverse dynamic analysis." J Biomech 28(10): 1179-91.
- Hardt, D. E. (1978). "Determining Muscle Forces in the Leg During Normal Human Walking Em Dash an Application and Evaluation of Optimization Methods." J Biomech Eng Trans ASME 100: 72-78.
- Hatze, H. (1980). "A mathematical model for the computational determination of parameter values of anthropomorphic segments." J Biomech 13(10): 833-43.
- Hinrichs, R. N. (1985). "Regression equations to predict segmental moments of inertia from anthropometric measurements: an extension of the data of Chandler et al. (1975)." J Biomech 18(8): 621-4.

- Huang, H. K. and S. C. Wu (1976). "The evaluation of mass densities of human body in vivo from CT scans." Comput Biol Med 6(4): 337-43.
- Jensen, R. K. (1978). "Estimation of the biomechanical properties of three body types using a photogrammetric method." J Biomech 11(8-9): 349-58.
- Jensen, R. K. (1989). "Changes in segment inertia proportions between 4 and 20 years." J Biomech 22(6-7): 529-36.
- Kane, T. R. and D. A. Levinson (1985). Dynamics, theory and applications. New York, McGraw-Hill.
- Krabbe, B., R. Farkas, et al. (1997). "Influence of inertia on intersegment moments of the lower extremity joints." J Biomech 30(5): 517-9.
- Ladin, Z. and G. Wu (1991). "Combining position and acceleration measurements for joint force estimation." J Biomech 24(12): 1173-87.
- Lubich, C., C. Engstler, et al. (1995). "Numerical integration of constrained mechanical systems using MEXX." Mechanics of Structures and Machines 23: 473-495.
- Martin, P. E., M. Mungiole, et al. (1989). "The use of magnetic resonance imaging for measuring segment inertial properties." J Biomech 22(4): 367-76.
- Meirovitch, L. (1970). Methods of analytical dynamics. New York, McGraw-Hill.
- Mungiole, M. and P. E. Martin (1990). "Estimating segment inertial properties: comparison of magnetic resonance imaging with existing methods." J Biomech 23(10): 1039-46.
- Ozkaya, N. and M. Nordin (1991). Fundamentals of biomechanics : equilibrium, motion, and deformation / TMzkaya, Margareta Nordin. New York, Van Nostrand Reinhold.
- Patriarco, A. G., R. W. Mann, et al. (1981). "An evaluation of the approaches of optimization models in the prediction of muscle forces during human gait." J Biomech 14(8): 513-25.
- Sarfaty, O. and Z. Ladin (1993). "A video-based system for the estimation of the inertial properties of body segments [see comments]." J Biomech 26(8): 1011-6.
- Shen, W. (2000). Gait3D User's Manual: Version 1.0. San Diego, CA, Jaycor, Inc: 35.
- Soderkvist, I. and P. A. Wedin (1993). "Determining the movements of the skeleton using well-configured markers." J Biomech 26(12): 1473-7.
- Spoor, C. W. and F. E. Veldpaus (1980). "Rigid body motion calculated from spatial co-ordinates of markers." J Biomech 13(4): 391-3.
- van den Bogert, A., L. Read, et al. (1996). "A method for inverse dynamic analysis using accelerometry." J Biomech 29(7): 949-54.
- Vaughan, C. L., B. L. Davis, et al. (1990). Dynamics of human gait. Champaign, Illinois, Human kinetics Publishers.
- Vaughan, C. L., J. G. Hay, et al. (1982). "Closed loop problems in biomechanics. Part II--an optimization approach." J Biomech 15(3): 201-10.
- Veldpaus, F. E., H. J. Woltring, et al. (1988). "A least-squares algorithm for the equiform transformation from spatial marker co-ordinates." J Biomech 21(1): 45-54.
- Winter, D. A. (1990). Biomechanics and motor control of human movement. New York, John Wiley & Sons, Inc.
- Yeadon, M. R. and M. Morlock (1989). "The appropriate use of regression equations for the estimation of segmental inertia parameters." J Biomech 22(6-7): 683-9.
- Zatsiorsky, V. M. and V. N. Seluyanov (1985). Estimation of the mass and inertia characteristics of the human body by means of the best predictive regression equations. Biomechanics IX-B. D. A. Winter. Champaign, IL, Human Kinetics Publisher: 233-239.

Zatsiorsky, V. M., V. N. Seluyanov, et al. (1990). In vivo body segment inertial parameters determination using a gamma-scanner method. Biomechanics of Human Movement: Application in Rehabilitation, Sports and Ergonomics. Ohio, Bertec Corporation: 186-202.

